CONDITION ASSESSMENT OF CARBON FIBER COMPOSITES USING RAMAN SPECTROSCOPY

A Thesis Presented to the Faculty of the Graduate School of the

University of Missouri - Columbia

In Partial Fulfillment of the Requirements for the Degree

Master of Science

By

Frank D. Blum, Jr.

Dr. Glenn Washer, Graduate Advisor

JULY 2009

The undersigned, appointed by the Dean of the Graduate School, have examined the thesis entitled

CONDITION ASSESSMENT OF CARBON FIBER COMPOSITES USING RAMAN SPECTROSCOPY

Presented by Frank D. Blum, Jr.,

A candidate for the degree of Master of Science,

And hereby certify that, in their opinion, it is worthy of acceptance.

Professor Glenn Washer

Professor John Bowders

Professor Roger Fales

ACKNOWLEDGEMENTS

I would like to thank my advisor, Dr. Glenn Washer, Assistant Professor of the Department of Civil and Environmental Engineering at the University of Missouri-Columbia. Dr. Washer's knowledge and supervision were critical in all of the progress made on this project and in my development as a graduate student.

For their expertise and generosity in equipment use I would like to thank Dr. Steve Martin, Professor in the Department of Materials Science and Engineering at Iowa State University, and Dr. Shubhra Gangopadhyay, Professor in Electrical Engineering at the University of Missouri-Columbia. In addition to these individuals I would like to express my gratitude to their research staff and graduate students whom helped me during testing.

I would also like to thank Brian Samuels and Rex Gish and the rest of the Engineering Technical Services (ETS) for their skill and technical assistance in fabricating components for this project. Additionally I would like to thank a number of graduate and undergraduate students who have helped me during my graduate work. Naveen Bolleni, Tommy Brooks, Patrick Earney, Richard Fenwick, Grant Luckenbill, Scott Morris, Seth Nelson, and Caleb Philipps all have provided me with assistance in my research and graduate studies.

Finally, I would like to give my sincere appreciation to the American Society of Non-destructive Testing (ASNT) for funding this project and my graduate studies.

TABLE OF CONTENTS

LIST OF FIGURES

LIST OF TABLES

ABSTRACT

The goal of this research is to examine the potential of Raman spectroscopy as a method of condition assessment for carbon fiber composite materials. Carbon fiber composites are used in high performance situations such as overwrapping of composite over-wrapped pressure vessels (COPVs) in aerospace applications and hydrogen and natural-gas transportation systems. The composites will play a larger role in the future due to the materials high strength to mass ratio. There are currently limited nondestructive evaluation (NDE) technologies to evaluate these composite materials in-situ. NDE technologies will be critical for analyzing environmentally caused degradation that can reduce strength and service life of the materials. Variations in elastic strain in the composite material can manifest from degradation or damage, and can be analyzed using Raman spectroscopy. The characterization of active Raman bands and the strain sensitivity of these bands for commercially available carbon fibers are reported. Additionally carbon fiber/epoxy matrix strands and burst COPV samples are investigated. These results indicate that Raman spectroscopy has some ability to make strain measurements in commercially available carbon fibers. Such measurements have the potential to be used as a tool for NDE in inspections and reliability assessment of carbon fiber composite materials.

1 INTRODUCTION

1.1 Background

The role of carbon fiber is increasing in the world due to its high performance characteristics provided by its high strength to weight ratio. Additionally, as the cost of production goes down and performance characteristics go up, new applications are appearing at a rapid pace. These fibers are sometimes used on their own, but are more commonly used as reinforcement of a composite material, often pairing the fiber with epoxy to create a matrix. Currently there are many applications including bicycles, sporting goods such as tennis racquets and golf clubs, commercial and military aircraft, high-end automobiles and their components, and applications in the transportation and aerospace industry. The focus of the research reported here is of fiber-epoxy composites used in the transportation and aerospace industries.

Carbon fiber-epoxy composites are a type of composite over-wrapped pressure vessels (COPV) and are commonly used as the wrapping material of lightweight hydrogen fuel tanks. The carbon fiber/epoxy matrix composite over-wraps a metal or plastic liner and takes the load when the vessels are pressurized. The composite material may be exposed to prolonged periods of stress and environmental degradation. These stresses and degradation are

typically not visible and a (Non-destructive Evaluation) NDE method to asses the vessels is needed. Currently these COPVs must be monitored using life cycles and temperature limits. The use of these pressure vessels will likely increase as the hydrogen economy is expanding as a possible cleaner and cheaper solution for fuel. These vessels will be present in hydrogen vehicles and their supporting facilities such as fueling stations, storage containers, and pipelines. Additionally, vessels of this type are present on NASA vehicles due to their high strength to weight ratio and as research increases, these vessels should be a solution for high performance materials. There are currently few methods to evaluate these materials non-destructively except for the human eye.

1.2 Goal

The goal of this project is to examine the potential of Raman spectroscopy to be used as a non-destructive means of condition assessment for carbon fiber composite material. Raman spectroscopy uses light scattering to investigate material at their molecular interaction level. In many fields Raman spectroscopy is a powerful materials characterization tool, and with new, more compact technologies and testing methods, its range of applications will likely increase. Previous research on carbon fiber and carbon materials in general have provided insight as to relating distinct features in Raman measurements to carbon-carbon bond interaction. Investigating differences in Raman spectra could give information about fiber material characteristics such as modulus and tensile strength, as well as the amount of stress the composite material is under.

1.3 Objectives

There are a number of objectives in this project.

- Measure different types of raw carbon fiber and to characterize their Raman spectra produced, highlighting active Raman bands.
- Investigate the sensitivity of peak location shifting with applied strain on the fibers.
- Further analyze Raman band characteristics with applied strain by looking at relative band intensity ratios and full-width-at-half-maximum (FWHM) ratios.
- Characterize the spectra of composite materials and investigate their strain sensitivity.
- Determine the Raman potential of making measurements on material directly from COPVs and the ability to penetrate different surfaces/coatings for these measurements.

These exploratory tests on carbon fibers and their composites will provide a basis for further investigation utilizing Raman spectroscopy as tool for condition assessment.

1.4 Scope

Both pitch and Polyacrylonitrile (PAN)-based carbon fibers are investigated at different incident laser wavelengths in order to develop ideal testing scenarios. This process was also carried out for the carbon fiber composite material; both fiber/epoxy strands and material ripped directly from COPVs. The composite material is more difficult to work with due to the added

complexity of the material but is more indicative of materials being used in the field today.

In addition to acquiring spectra for the materials, strain testing was carried out for all the raw fibers and the composites materials that were able to be placed in a load frame. The load frame is able to apply uniaxial tension in the direction of the fiber axis. Spectra were obtained at various strain levels within the elastic range of the materials to investigate the potential peak location shift with applied tensile strain. The fibers and composites are evaluated not only with respect to their Raman band location, but also their full-width-at-half-maximum and intensity ratios of the Raman bands relative to a reference Raman band. These two properties allow for quantifiable analysis of the Raman bands beyond just that of peak location.

For materials provided from failed COPVs it is of importance to investigate the potential for Raman spectroscopy to penetrate the outer coating of the material to look at the spectra of the fiber component underneath the surface. Laser wavelengths and accumulation parameters can be adjusted in many ways to develop a potential non-destructive method to analyze these composite materials.

2 BACKGROUND

2.1 Carbon Fiber

2.1.1 Overview

Carbon fibers are thin fibers smaller than a human hair, ranging from 5 to 10 microns in diameter that contain at least 92% carbon by weight. The structure of a carbon fiber can be crystalline, amorphous, or a combination of both. Carbon atoms have an ability to form bonds between atoms to create stable compounds in the forms of chains and rings. Graphite and diamond are the two most common allotropes of carbon and are able to form into effectively infinite networks of atoms. For most carbon fiber, the structure consists of layers of one-atom-thick sp^2-bonded carbon atoms organized hexagonally (honeycomb crystal lattice) known as graphene layers, with van der Waals bonding between layers to make a three dimensional structure. Figure 2.1 shows a graphene layer. Carbon fibers are able to achieve their high modulus because the honeycomb carbon layers are oriented parallel to the fiber axis. Fibers generally have a much higher modulus and strength in the direction of the fiber axis than perpendicular to the it [1]. Differences in structure and material composition depend on production methods and the type of precursor used for the fiber, which will be discussed later.

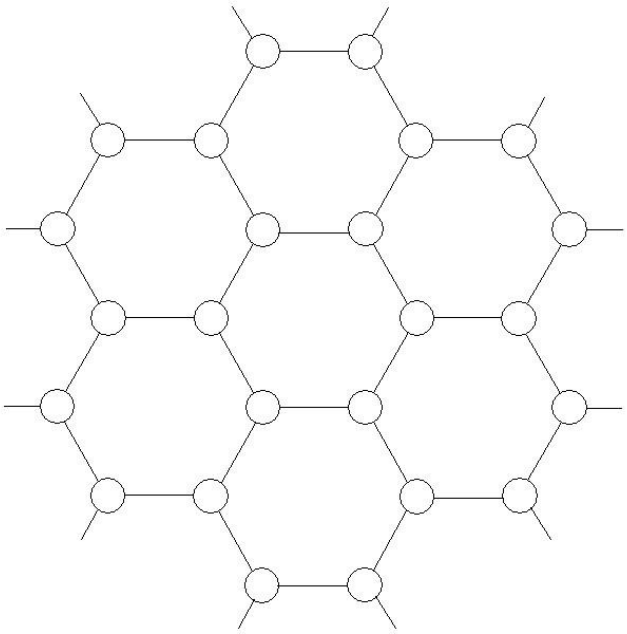

Figure 2-1. Graphene layer in which carbon atoms are organized in a hexagonal lattice.

The first high-performance carbon fibers were graphite whiskers developed in 1958 by Union Carbide scientists in Cleveland, OH. The fibers were derived using Rayon as a precursor and only contained 20% carbon [2]. Graphite whiskers have the carbon layer rolled up like a scroll and are derived from a single crystal. Graphite whiskers are near flaw-free and very high in strength, but are not commercially relevant due to their low production yield [1]. Fibers today, and those investigated in this report, are typically polyacrylonitrile (PAN) and pitch-based carbon fibers. Typical high-performance fibers today, such as Toray's T1000® PAN-based fiber, can have a Young's modulus of 300 gigapascals (GPa) and a tensile strength of 7 GPa. In addition to their high strength to weight ratio, carbon fibers have many desirable qualities including low

thermal expansion, low electrical resistivity, high creep resistance, high thermal conductivity, and corrosion resistance. One downside of carbon fibers is their low ductility, which is a larger concern the higher modulus the fibers. Historically carbon fiber has not been as developed as other technologies due to the high manufacturing costs, but recently with the increase in applications and market size the prices of carbon fibers have lowered.

2.1.2 PAN-based

Polyacrylonitrile (PAN) based fibers are currently the most popular type of carbon fiber used today. PAN is an organic polymer composed of a mixture of acrylonitrile (CH_2=CHCN) as the main component, mixed with other monomers. PAN contains a continuous carbon backbone that is ideal for the processes required to convert PAN to the final product of carbon fiber. [3]

Converting PAN to carbon fibers is a multi-step process that can be altered to manufacture fibers of desired specifications. The PAN is first fabricated into shape by wet spinning techniques. Then, generally, the next step is to oxidize the PAN by heating it to about 300 °C in air. Acrylonitrile has a carbon content of 67.9%, allowing for PAN precursors to have a carbon yield of 50-55% after the initial heating that eliminates hydrogen and adds less volatile oxygen to the PAN. During this process the polymer changes from a long chain form of polyacrylonitrile known as a ladder to more stable ring structures. The oxidized PAN is then heated in a chamber along with an inert gas such as argon to temperatures as high as 3000 °C in a process called graphitization. Graphitization changes the molecular structure by burning off non-carbon

material, and as the level of graphitization increases, non-crystalline carbon layers stack onto the crystalline regions. The higher the level of graphitization, the higher the amount of ordered, crystalline carbon, allowing for higher grade fiber to be produced [4]. Under ideal conditions the carbon content can reach 93-95% for carbon fibers, and 99% to be classified a graphite fiber. PAN based fibers are able to achieve high modulus, high strength characteristics [3].

2.1.3 Pitch-based

Pitch is a resinous liquid that appears as a solid that can be made from petroleum products, coal, or plants. Pitch-based fibers have a smaller market share than PAN-based fibers, but it is currently increasing due to the lower cost/carbon content when compared to PAN-based. Pitch based carbon fibers have a higher carbon yield and molecular orientation in the direction of the fiber axis, giving the ability to produce much stiffer fibers. These fibers generally have a lower tensile strength than the PAN-based carbon fibers, partially due to their higher stiffness [1].

The process for making pitch fibers is very similar to the process for PAN fibers. The fibers are first produced during a process called melt spinning. During this spinning process the viscosity of the pitch is critical and very dependant on the spinning temperature [3]. After being spun the fibers go through the same stages of oxidation, carbonization, and graphitization as in the PAN-based fibers.

2.1.4 Carbon Fiber Composites

Carbon fibers are most commonly used as the reinforcement component of a composite material. Composite materials refer to any engineered material using two or more materials with different physical properties. Carbon fibers high tensile strength and low density give them an exceptional ability to be used in composite materials.

One application for carbon fiber is the wrapping material in composite over-wrapped pressure vessels (COPVs) as shown in Figure 2-2. For this product, carbon fiber in long spools is mechanically wrapped around a bladder (usually metallic or polymer in nature) with viscous epoxy resin being applied at the same time. The result is a lightweight, polymer reinforcement with extremely high pressure ratings. Consumer COPVs can range as high as 10,000 psi, with specially engineered ones exceeding that.

Figure 2-2. Commercially available tough shell COPVs for gas storage manufactured by Lincoln Composites and published on the Lincoln Composites website.

2.1.5 Environmental Damage

As discussed in the goals of this project, there is a need for non-destructive evaluation (NDE) techniques for condition assessment of carbon fiber composite materials. While some failures will be obvious to the human eye, these materials can undergo long lifetime of service without any visual indication of wear and tear. Many environmental factors can lead to a reduction in strength properties in carbon fiber composites and service life of the material. Internally, composite materials have a complex matrix that is difficult to investigate with non-destructive methods. An NDE method of measuring the level of stress in carbon fiber composites would help in safety and engineering of these materials.

After a high impact collision of a composite material with a foreign object it may visually look in working condition, when in fact inside the polymeric matrix there are high amounts of damage. Impact damage to a composite material can crack composite matrix which can lead to fiber debonding from the epoxy material. When a fiber breaks, the load it carried is passed to adjacent fibers, sometimes causing them to fail in a chain reaction leading to catastrophic failure.

Another visually undetectable failure mechanism for composite materials is stress rupture. Stress rupture is a phenomenon in which the material has a large reduction in strength with a seemingly small addition of stress. The stress could come from an increase in COPV pressure or even from thermal loading, or a combination of the two. With long periods of sustained loading and cyclic loadings, COPVs are a composite material particularly prone to stress rupture and creep.

Polymeric materials can also be damaged by outside environmental conditions that induce changes to the structural integrity of the material. Exposure to ultraviolet radiation can change the molecular structure of the material and thus its strength characteristics. Hazardous chemicals can degrade the surface treatment and performance characteristics of the material. Finally, extreme temperatures can be very harmful to composite materials because they lead to residual strains from thermal expansion between the fibers and epoxy matrix.[3]

2.2 Raman Spectroscopy

Raman spectroscopy is a laser-induced technique that measures the intensity and frequency of inelastically scattered light and is used to study vibrational, rotational, and other low-frequency modes of interaction between molecules. The technique is named after Sir C.V. Raman, an Indian physicist who in 1928 discovered that inelastically scattered sunlight would change frequency as it passes through crossed filters [5]. From the Planck-Einstein equation, frequency is related to the energy of a particle by:

$$E = h \times f$$

where:

E = energy of a photon (m^2 kg / s^2)

h = Planck's constant (6.626 x 10^{-34} m^2 kg / s)

f = frequency of a photon (Hz)

Frequency and wavelength are inversely proportional to each other and related by the following equation:

$$f = \frac{v}{\lambda}$$

where:

f = frequency of a photon (Hz) or (1/s)

v = wave speed (m/s)

λ = wavelength (m)

In Raman spectroscopy, an incident laser sends photons (energy) to the material to be tested. Some photons scatter elastically (Rayleigh scattering) with the energy of the photons unchanged, while others shift wavelength and scatter inelastically (Raman scattering). The majority of photons are Rayleigh scattered, while typically the Raman scattering occurs weakly at an intensity of ~10^{-5} the incident beam [5]. During Raman scattering there is an energy transfer between the incident photons and the molecules, with the energy difference equal to the difference in the vibrational and rotational energy level between the incident photon and the material being tested. Figure 2.3 shows an incident photon interacting with a diatomic molecule and physically what happens during the Raman scattering process.

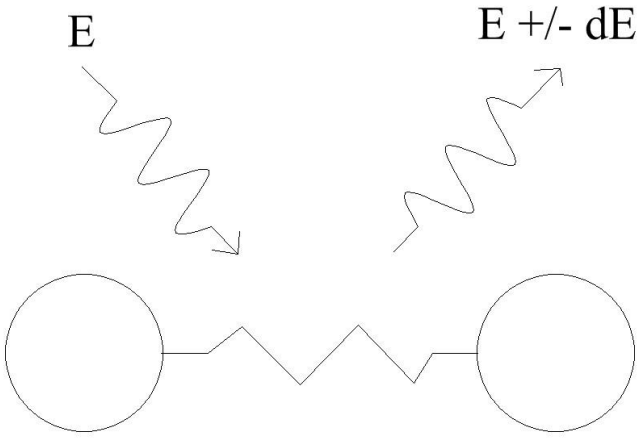

Figure 2-3. A diatomic molecule showing the Raman scattering process. Energy (via a photon) interacts with the molecule and is scattered at a different energy level.

Raman scattering can be divided into two types, Stokes and anti-Stokes. In Stokes scattering the material absorbs energy, thus resulting in photons of lower energy and a decrease in measured frequency. For anti-Stokes scattering the material loses energy and the photons are shifted to a higher energy level and frequency. The majority of materials absorb the induced photon energy and therefore Stokes scattering is typically at higher intensities then that of anti-Stokes [6]. Since both scattering types give the same information it is customary to measure only the Stokes side of the spectrum because of their stronger intensities [5]. Figure 2-4 shows the different types of scattering and their energy states.

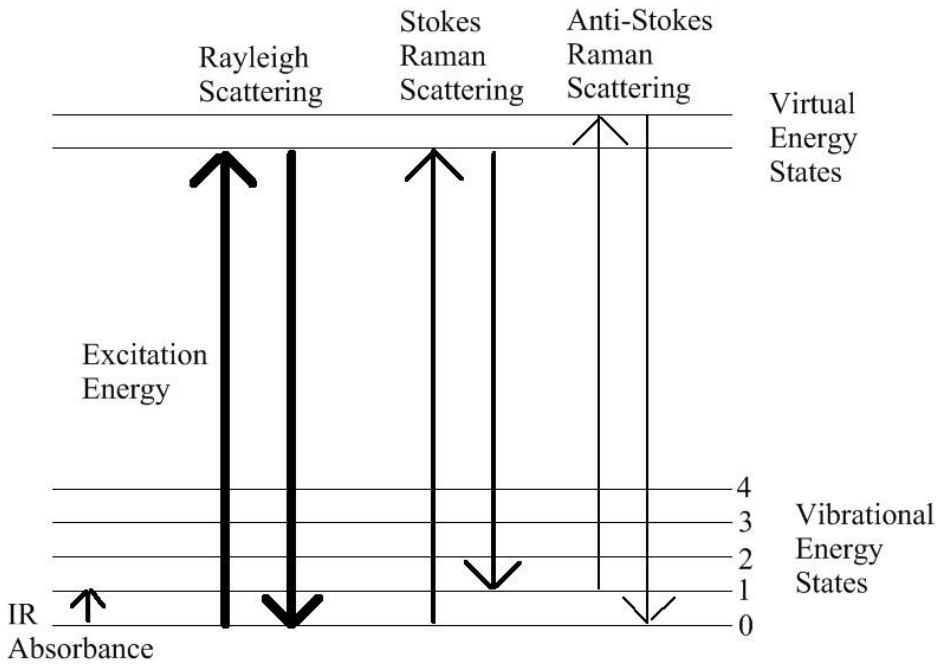

Figure 2-4. An energy level diagram of different energy types of scattering during the Raman process.

In Raman spectroscopy a measurement of the vibrational frequency, as a shift from the incident beam frequency, is made. These frequencies are usually reported in wavenumbers as shown in Figure 2-5. The inelastically scattered light, v_1, is subtracted from the incident light, v_0, to calculate a relative wavenumber, v_r. The equation for Stokes scattering is $v_r = v_0 - v_1$, while the equation for Anti-Stokes is $v_r = v_0 + v_1$.

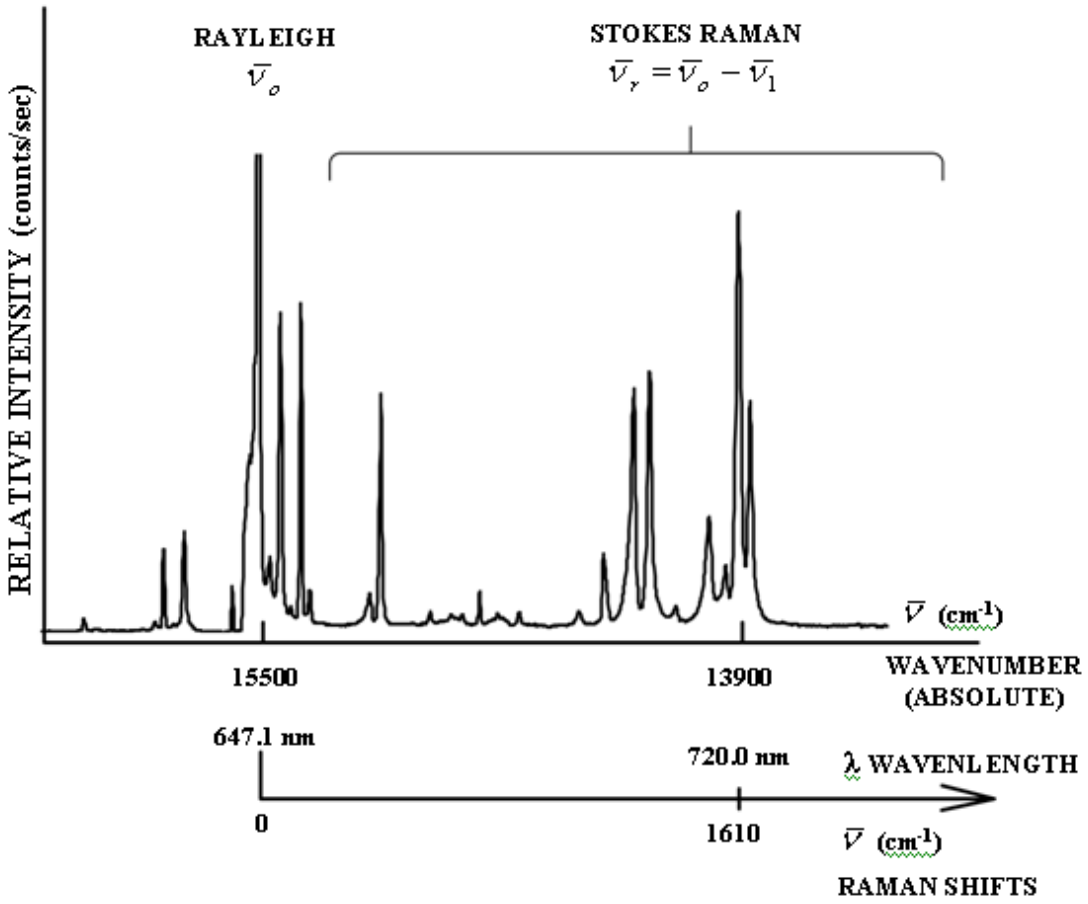

Figure 2-5. Illustration of converting absolute wavenumbers to Raman shifts [7].

As stated previously, the Raman shifts are dependent on material characteristics, specifically the molecular structure. The source of this scattering occurs when a molecule is irradiated by light which interacts with the electrons in bonds, causing an electric dipole moment to occur. The dipole moment is a product of the incident laser energy and the polarizability of the material. For a material to be Raman active it must exhibit change in polarizability as the vibration of the molecule changes. (The polarizability of a material changes as the electron clouds are deformed due to external energy, in this case the incident

light from the laser source.) The electric dipole excites molecules from an electronic ground state to a virtual energy state and back to a relaxed vibrational energy state as shown in Figure 2-4 [5]. These changes in energy, and thus frequency and wavelength, of the incident light when interacting with the material produce changes in the vibrational energy, producing Raman scattering. For example, vibrational frequencies associated with carbon-carbon double bonds produces specific Raman lines at well-defined frequencies relative to that of the incident radiation. Individual peaks can be associated with specific vibrational modes for molecules.

A typical Raman spectrometer schematic is shown in Figure 2-6. The sample is put underneath a microscope for focusing on an exact location of the material and illuminated using a fixed incident laser wavelength, typically between 488 and 1064 nm. Elastically scattered light is eliminated using notch filters, while the inelastically scattered light passes through a monochromator grating and is sent to the charge-coupled-device (CCD) detector. The CCD converts the Raman signal to an electrical output that can be stored to a computer. This value is then converted to a relative frequency (in wavenumbers), with the incident laser is set to zero value of Raman shift. The spectrometer is able to take measurements of the intensity of light reflected throughout a large frequency range, and is commonly investigated between 0 to 3200 cm^{-1} wavenumbers.

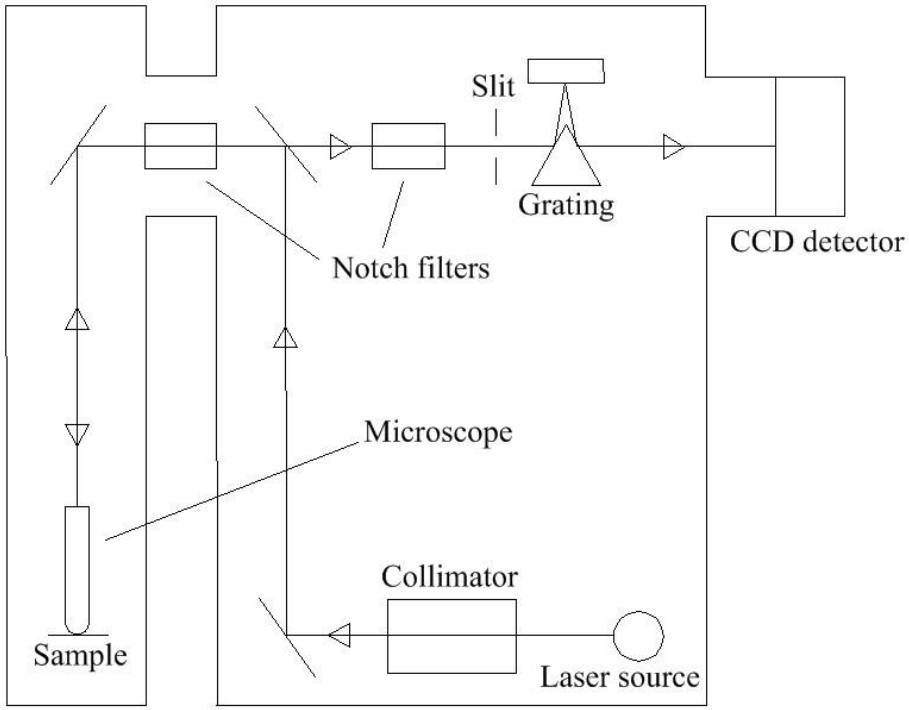

Figure 2-6. Schematic of a typical Raman spectrometer.

2.3 Raman Spectroscopy of Carbon Fiber

2.3.1 Raman Bands

Raman bands are sharp peaks that can be associated with vibration modes at a molecular level. Early studies on graphite materials revealed that a Raman band at the ~1585 cm^{-1} can be related to the vibration mode denoted by the symmetry classification E_{2g} of a graphite cell restricting motion of the atoms to the plane of carbon atoms. This band is attributed to the virtually infinite hexagonally organized carbon-carbon bonded lattice structure of the graphene layers and is present in all carbon fibers. Another band in polycrystalline graphite was found at ~1355 cm^{-1}, and can be related to the A_{1g} vibration mode of the graphite plane and can be attribute to the symmetric boundaries of the graphite

crystals. Thus the ~1355 cm^{-1} band can be related to particle size and a structural disorder effect [8]. It is also found that the ~1355 cm^{-1} band is associated with poorly graphitized fibers and the band intensity will lower with fibers that have higher graphitization temperatures. This Raman band is commonly known as the "disorder" induced line and is more prevalent in low modulus/low heat treated fibers [9]. The letter designations of A_{1g} and E_{2g} are known as symmetric vibrational modes.

From literature there are several more Raman bands found in carbon fiber depending on the level of graphitization, laser power and wavelength, and source of material. For convenience, a letter notation is used to refer to the bands. The ~1355 and ~1585 cm^{-1} are assigned as D and G-lines respectively. The strong G-line is present due to the hexagonal ring structure with E_{2G} symmetry of graphite crystal. The weak D-line is of A_{1G} symmetry and is present in disordered forms of carbon. At low firing temperatures, the D band will exhibit broad lines [10, 11]. For non-graphitized fibers, a D'-line is present at ~1620 cm^{-1}. At higher firing temperatures it can be detected as a shoulder of the G-line. An overtone of the D-line is present at ~2720 as the G'-line. Although it is present as an overtone of the D-line, it is more closely linked to Raman characteristics such as intensity and FWHM to the G-line [9]. Another band present is the G''-line at ~2950 cm^{-1}, often referred to as a combination band, at a frequency roughly the sum of the D and G-lines is likely a combination of the two [12]. As previously stated, different fibers and composites will contain additional bands due to their material characteristics.

Table 2-1. Location and details of major Raman bands associated with carbon fiber.

~ Peak Location (cm^{-1})	Notes
1355, D-band	Breakdown of lattice symmetry with A_{1g} vibrational mode of the graphite plane
1585, G-band	Single graphite crystals with E_{2g} vibrational mode of the graphite cell
1620, D'-band	Non-graphitized fibers and detected as a shoulder of the G-band
2720, G'-band	Overtone of the D-band
2950, G''-band	Overtone combination of both the D and G-bands

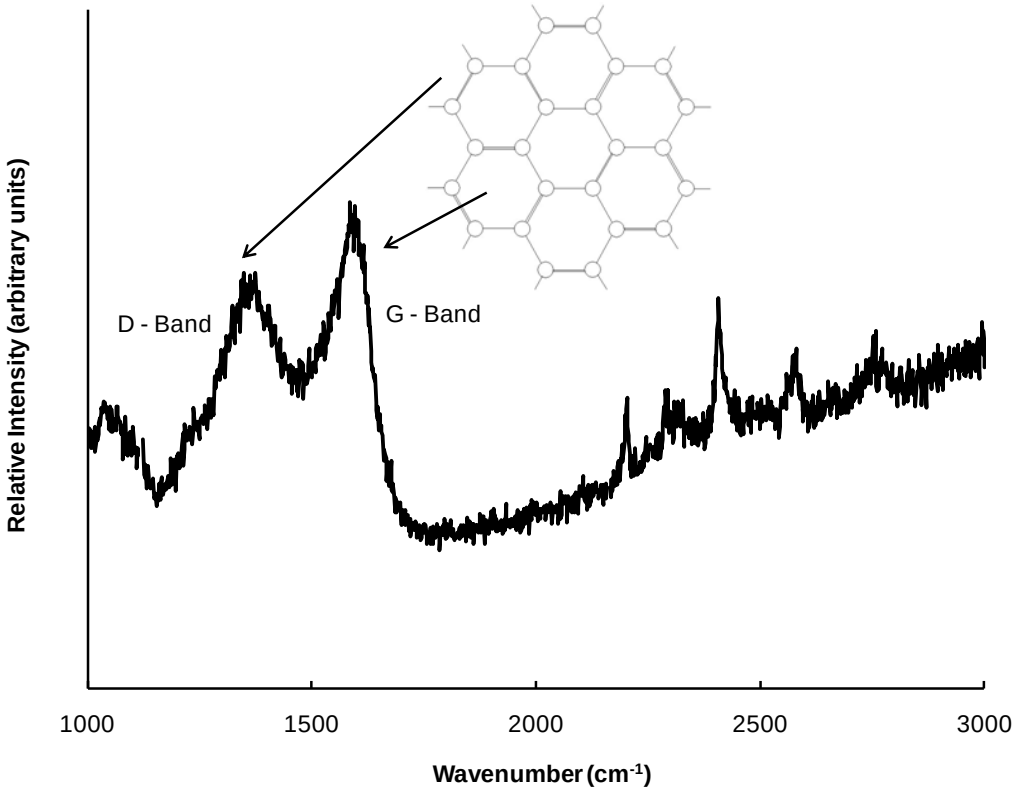

Figure 2-7. Raman spectra of carbon fiber showing the G-band attributed to a single graphite crystal and the D-band associated with structural disorder of the crystal lattice.

2.3.2 Strain Dependence

It has been found from previous research that Raman bands present in the spectra of carbon fiber are strain sensitive [13]. With an increase in applied tensile strain, Raman bands shift to lower frequencies and tend to broaden in width [14, 15]. Conversely, with applied compressive strain the Raman bands will shift to higher frequencies [16]. The principal reason to these frequency shifts with applied strain is due to bond anharmonicity, particularly in the carbon-carbon double and triple bonds. Anharmonicity refers to a deviation of a system from being a harmonic oscillator, and in molecular physics occur when there is displacement between two atoms due to an external force. In carbon fiber this displacement causes change in molecular lattice structure and vibrations. These bond anharmonicities lead to a decrease in bond modulus and vibrational frequencies with an increasing stress [17]. For carbon fibers, the shift for a Raman band is dependent upon the fiber modulus, with stiffer fibers exhibiting a larger frequency shift. The slope of this linear relationship is referred to as the Raman frequency gauge factor (RFGF). The RFGF has been found to increase as the Raman band investigated is greater in frequency [18]. So for the same fiber, the RFGF value will increase from the D-line to the G-line to the second-order Raman bands [16]. For the G-line at 1585 cm^{-1}, frequency shifts (RFGF) have been found on the order of 10 cm^{-1} / % applied strain for PAN-based fibers and 12 cm^{-1}/ % applied stain for pitch-based fibers [14, 18].

The RFGF has the potential to contribute to the condition assessment of the carbon-wrapped COPVs by providing engineering knowledge of the state of

stress in the surface of COPVs as a means of detecting damage or degradation of the COPV. Initial measurements are reported here to provide foundational data on the Raman response of commercially available fibers in their as-marketed conditions.

3 EXPERIMENTAL

3.1 Instrumentation

The Raman spectra in this report are measured using two different Renishaw micro-Raman systems and a Fourier Transform (FT) Raman system. The variation of the systems allowed for measurements to be taken at 488, 514, 647, 752, and 1064nm incident wavelengths. The use of different wavelengths allows for different sample penetration abilities when taking measurements.

For the Renishaw micro-Raman systems, the incident wavelength is focused on the fiber/composite using a 20x, 25x, or 50x microscope. The Raman spectra of the illuminated fibers are collected over a time period using a CCD to collect the intensity of light reflected from the surface of the fibers over a range of wavelengths. The range of wavelengths collected was typically from 1000 to 3000 cm^{-1} over a time period of at least 50 seconds and multiple accumulations for high sensitivity. The spectral resolution of the system varies from 1.0 - 1.7cm^{-1} depending on the incident laser and optical alignments. The Renishaw spectrometers are calibrated using a silicon sample due to its well defined peak at 520 cm^{-1}.

Figure 3-1. Multi-laser Renishaw Raman spectrometer.

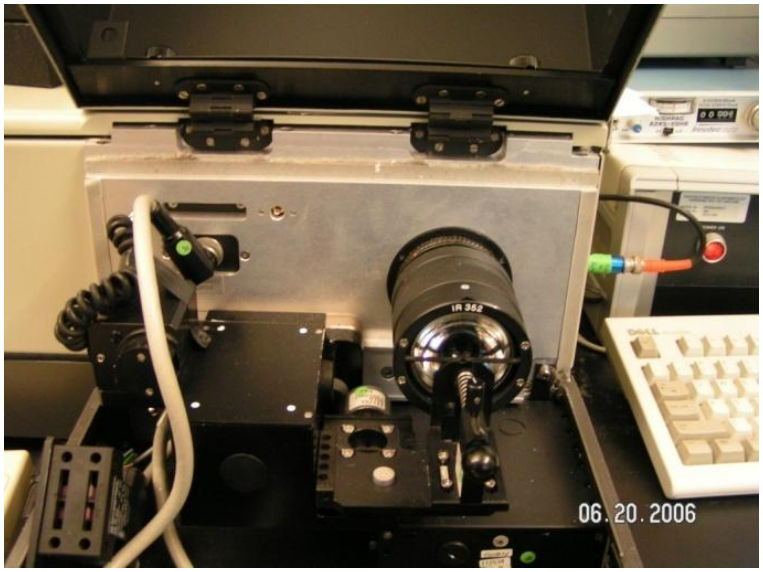

Figure 3-2. Fourier Transform (FT) Raman spectrometer.

3.2 Materials Tested

3.2.1 Raw Fibers

For the exclusive characterization of the carbon fiber's Raman spectra, many raw fibers were evaluated. Raw carbon fibers were supplied from various sources and manufacturers and include both PAN and pitch based fibers. Table 3-1 lists each of the fibers tested and their critical properties.

Table 3-1. Mechanical Properties of Carbon Fibers tested.

Fiber Type	Tensile Modulus		Tensile Strength		Elongation	Density
	GPa	Msi	MPa	Ksi	%	g/cm^3
Nippon (pitch)						
YS-95A	905	131	3497	505	0.3	2.20
CN-90	861	125	3384	489	0.4	2.19
CN-80	794	115	3138	453	0.5	2.17
CN-60	635	92	3189	460	0.6	2.12
Toray (PAN)						
T700	230	33.4	4900	711	2.1	1.80
T1000	294	42.7	6370	924	2.2	1.80
Cytec (PAN)						
T300	231	33.5	3650	529	1.4	1.76

The Nippon Graphite Fiber Corporation supplied fibers are high-modulus pitch based carbon fibers. The fibers from Nippon are technically graphite fibers due to their material composition being 99% or above carbon. The fibers high ordered carbon content is very crystalline and gives the product high stiffness. The Toray Carbon Fiber samples are PAN-based fibers. The T700S fiber is a high strength, standard modulus fiber typically used in pressure vessels. The T700S fiber was provided by Lincoln Composites, manufacturers of commercial TuffShell fuel tanks used for hydrogen and natural gas storage. A Lincoln

Composites plant tour in Lincoln, NE was given to help understand the pressure vessel manufacturing process. The T1000 fiber is ultra-high strength and used in critical applications such as aerospace pressure vessels. Also tested was a high strength, high strain, PAN based, surface treated T300 fiber from Cytec Corporation. For better understanding of the material tested, images of samples were prepared using a scanning electron microscope.

Figure 3-3. Nippon Graphite Fibers samples from top left clockwise, CN60, CN80, YS-95A, and CN90.

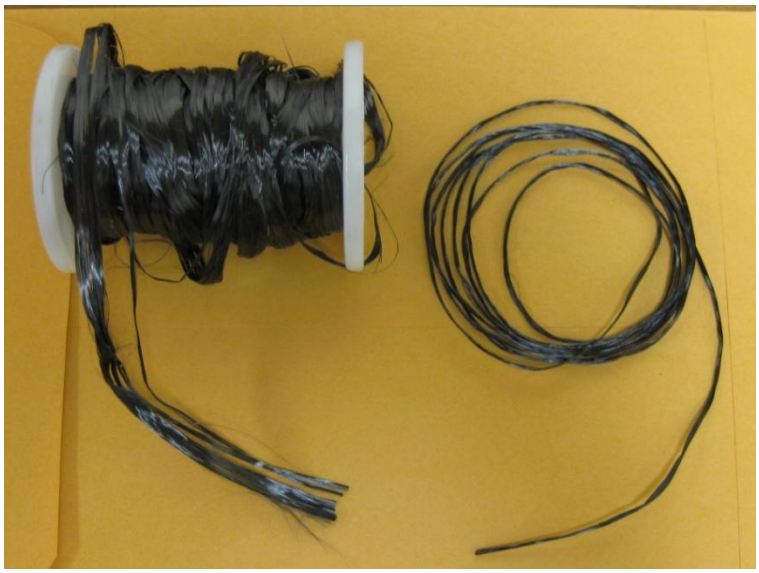

Figure 3-4. Spool of T700 fiber (left) and a section of T1000 fiber (right).

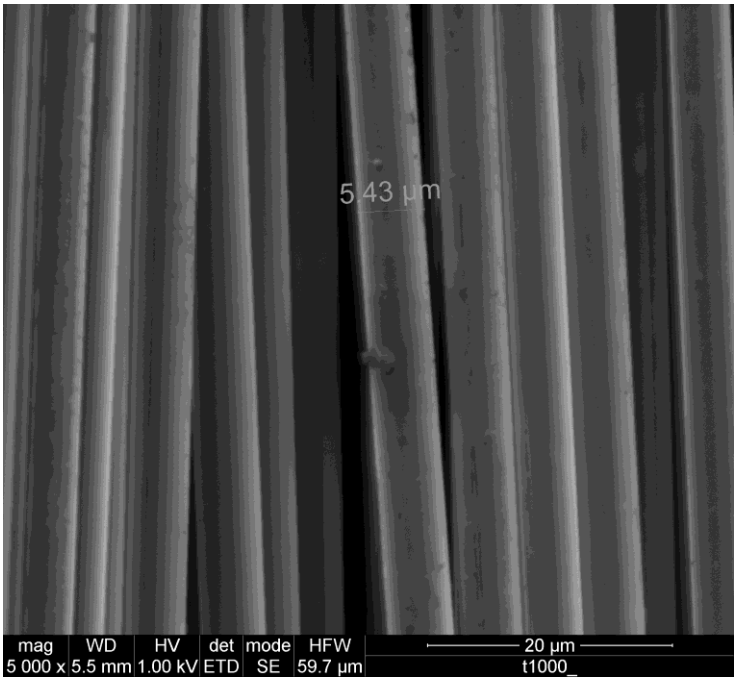

Figure 3-5. Image of T1000 carbon fiber at 5000x using an electron microscope.

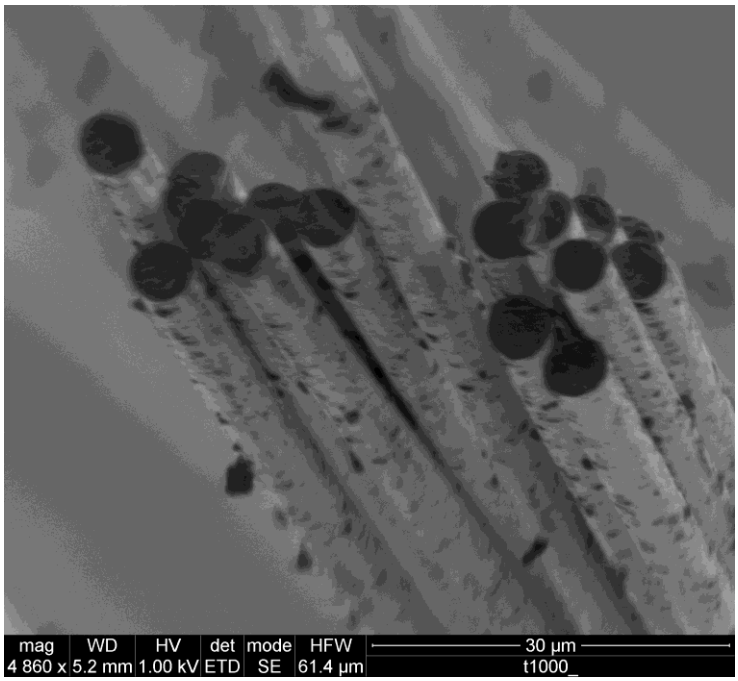

Figure 3-6. Image of T1000 carbon fiber at 4860x using an electron microscope.

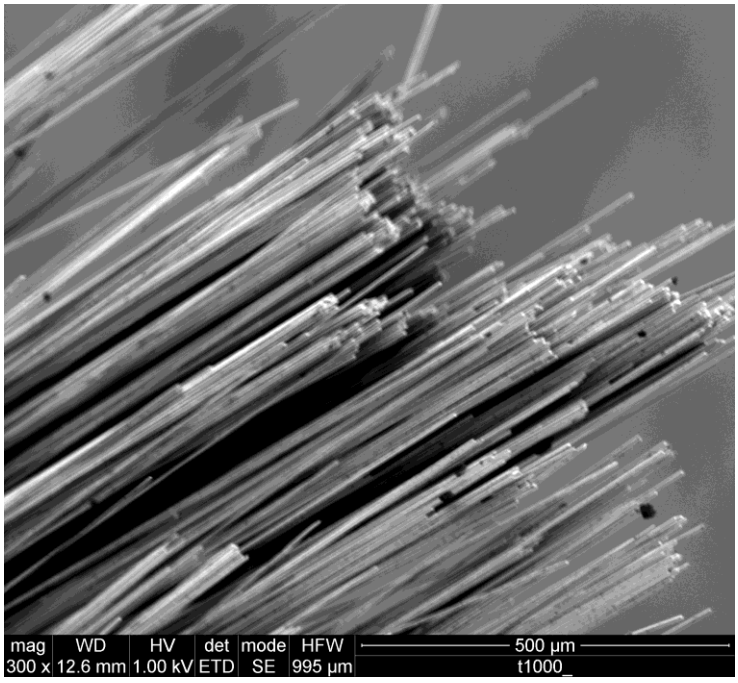

Figure 3-7. Image of T1000 carbon fiber at 300x using an electron microscope.

3.2.2 Fiber/Epoxy Composites

In addition to raw fiber samples, fiber/epoxy composite samples were tested. It is important to be able to measure the Raman spectra of carbon fiber in-situ, so the first step is to establish the ability to measure them in their composite application form. These composites range from pre-preg strands from the manufacturers to in-house made fiber/epoxy composite strands. Table 3-2 lists the composite materials tested. The Toray T1000/epoxy pre-preg and Hexcel IM7/epoxy pre-preg samples were sent along with burst COPVs (to be discussed in following section) as a sample of the material used in wrapping the COPVs. Pre-preg materials are large groupings of fibers with epoxy matrix material on the material that activates when heated up to bond the fibers and form a composite material. The Hexcel AS4 was sent as a manufactured fiber/epoxy strand. For the Nippon Graphite fibers, strand was made in-house using a Devco brand quick-epoxy.

Table 3-2. Types of Fiber/Epoxy composites tested.

Sample Type	Notes
Toray T1000/epoxy pre-preg	control sample for burst tank
Hexcel IM7/epoxy pre-preg	control sample for burst tank
Hexcel AS4	manufactured strand
Nippon Graphite Fibers/quick epoxy	in-house manufactured strand

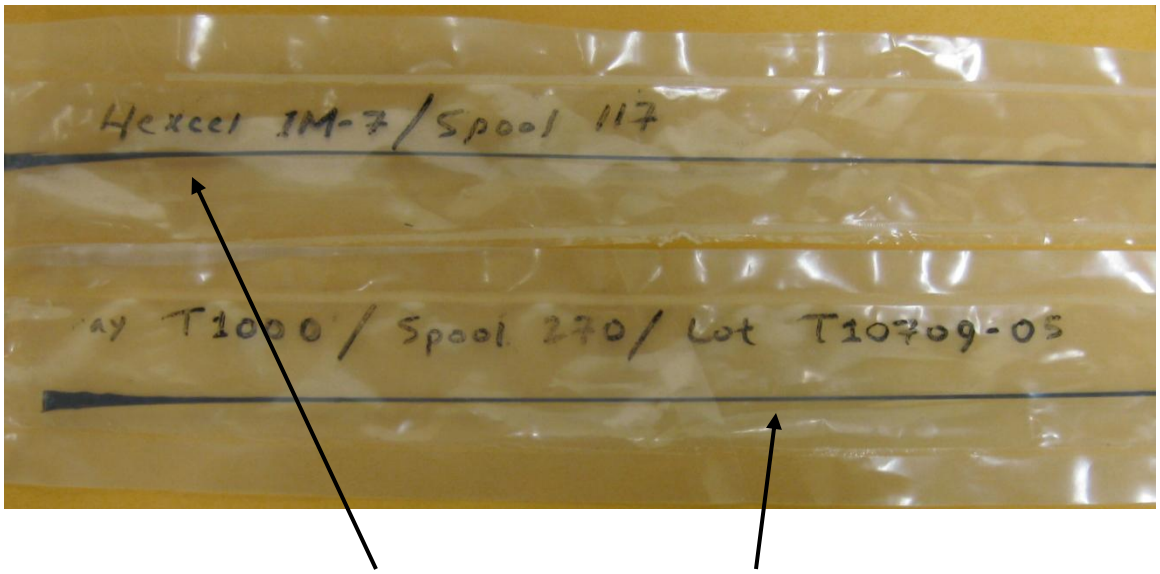

Figure 3-8. Image of Hexcel IM-7 spool (top) and Toray T1000 spool (bottom).

3.2.3 Composites from Burst Tanks

The composite materials tested from burst tanks were provided by NASA in the form of small sample pieces and also two separate failed tanks themselves. Samples of T-40 Fiber/Epoxy matrix wrapping ripped from a burst tank were sent for measurement. The T-40 fiber is a fiber with enhanced tensile strength and modulus specifically designed for aerospace applications. Two different types of burst (failed) COPVs were supplied for testing the ability of Raman to penetrate coatings. One tank is a T1000/epoxy wrapping that is shiny in exterior appearance that is shown in Figures 3-9 and 3-10. The other tank is an IM7/epoxy composite with a peal-ply treatment on the outside of the tank and is shown in Figures 3-11 and 3-12. Peal-ply is an adhesive polymer material that is put on the outer surface of a tank and then ripped off to leave a uniform finish and get rid of discontinuities that may arise during the fiber wrapping and epoxy coating process. The tanks were cut into small pieces that could be set

underneath the Raman laser. Investigation of both the outer surface of the tanks and the inner fiber/epoxy matrix parts was conducted.

Table 3-3. Types of composites tested from burst tanks.

Sample Type	Notes
T-40 fiber/epoxy	Pieces ripped from burst tank
T1000 fiber/epoxy burst tank	Samples cut from burst tank
IM7 fiber/epoxy with Peal-Ply burst tank	Samples cut from burst tank

Figure 3-9. Image of T1000/epoxy burst COPV.

Figure 3-10. Zoom-in image of T1000/epoxy wrapping material of COPV.

Figure 3-11. Zoom-in image of burst tank with IM7/epoxy with peal-ply treatment on the outer surface.

Figure 3-12. Zoom-in image showing peal-ply treatment.

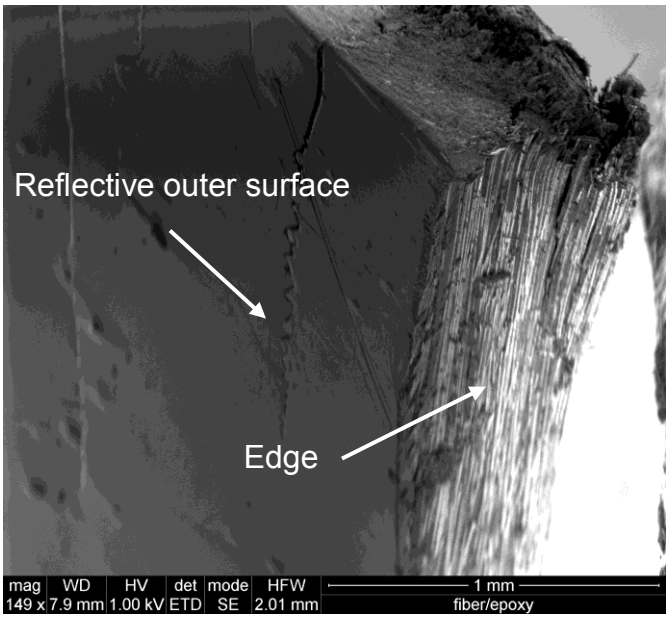

Figure 3-13. Image of T1000/epoxy piece from a burst COPV at 149x using an electron microscope.

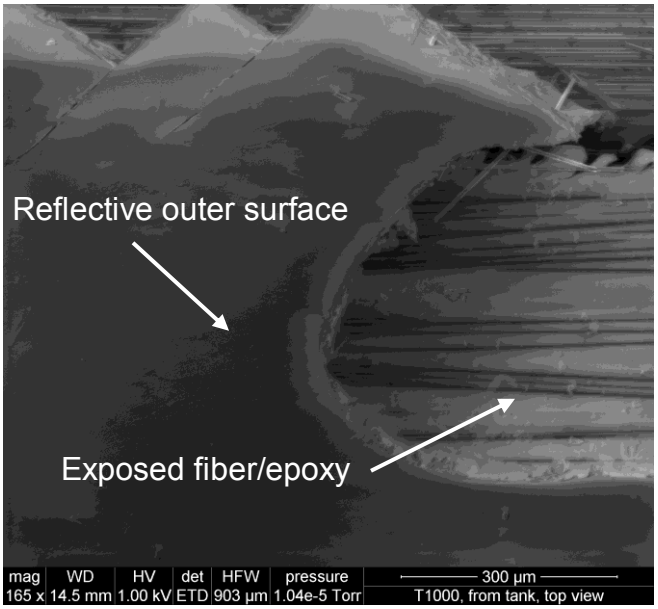

Figure 3-14. Image of T1000/Epoxy piece from a burst COPV at 165x using an electron microscope.

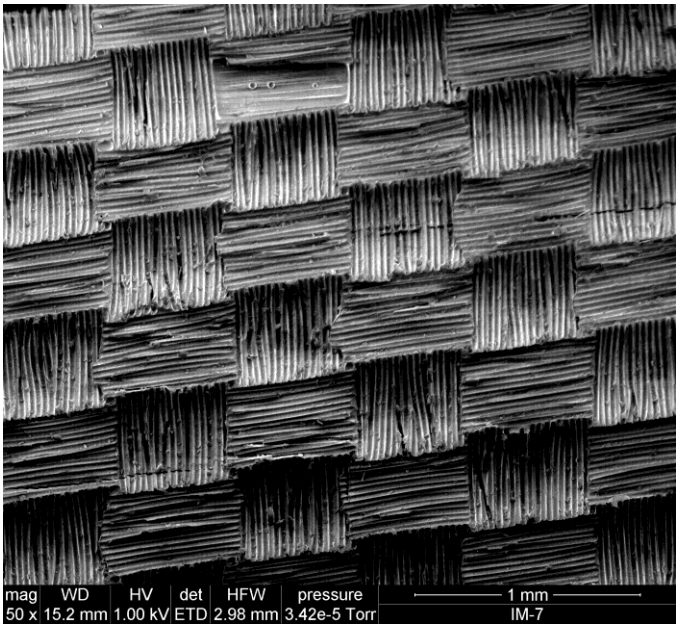

Figure 3-15. Image of IM7/epoxy outer surface with peal-ply material imprint on a burst COPV at 50x using an electron microscope.

3.3 Testing Methods

3.3.1 Set-up and Procedure

The carbon fibers and carbon fiber composite materials were tested using a variation of parameters to find optimal measurement conditions. Fibers were set underneath the laser of a certain known incident wavelength and power setting (schematic and Raman spectrometer physics were discussed in 2.2) and focused on the desired location using the built-in microscope. The microscope is able to focus on a circle with a diameter of as small as one micron. Measurements are taken over a specified range of wavenumbers in a specified number and lengths of accumulation. Generally, the higher the accumulation number and time the higher the sensitivity, or signal-to-noise-ratio, of the measurements taken. Higher power is also able to produce a cleaner signal,

but is very difficult to produce measurements at high power due to the likelyhood of fiber burnout, as shown in Figure 3-17, or saturation of the spectra produced resulting in extremely high intensities, weakening the relative sharpness of the Raman bands produced. For our samples typical spectral acquisition settings would be 2 accumulations of 50 seconds each at 10% power.

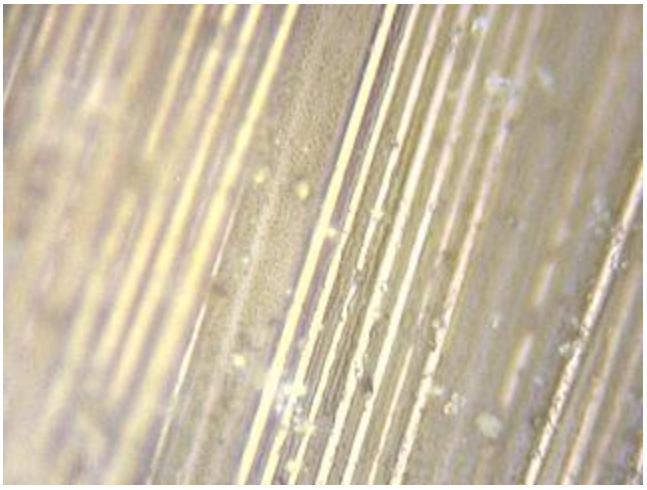

Figure 3-16. Image of T1000/epoxy matrix using a 50x microscope to focus on individual fibers.

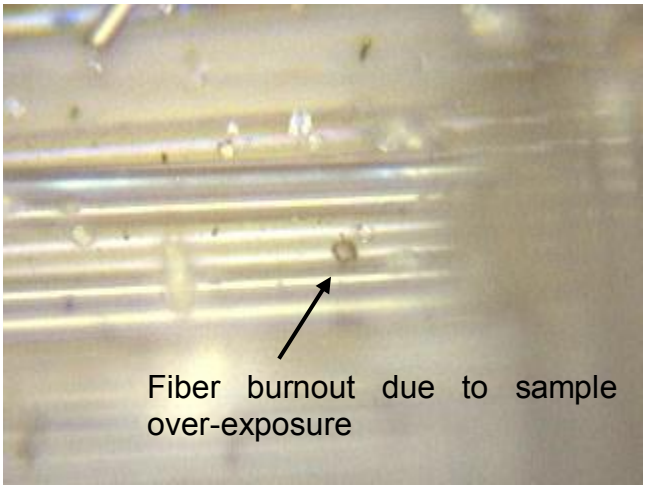

Figure 3-17. Image of IM7/epoxy with peal-ply treatment outer using a 50x microscope showing fiber burnout due to high power.

3.3.2 Strain Testing

For strain testing of the fibers and composite samples, in-house machined load frames were designed and fabricated. The first load frame was designed with an inline load cell to measure tensile force. The load cell was connected to a wireless node that provided data to a LabView® program recording voltage and was calibrated by hanging incremental weights to relate a measured voltage to a tensile force in pounds. A number of problems appeared with the load frame. The fibers tended to slip in the grips if not tightened enough, and crush and tear at those same points if tightened enough to prevent the slipping. With the fiber-epoxy matrix samples the grips tended to crush the sample and cause it to rip at the grip.

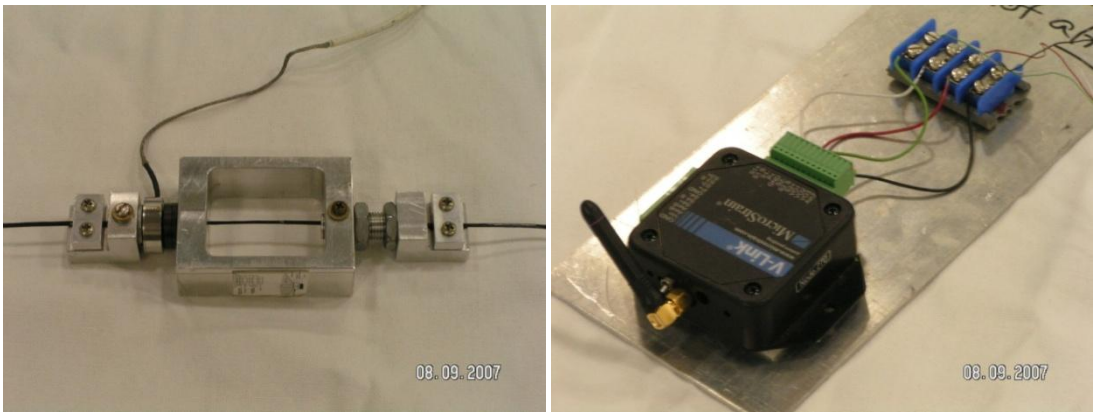

Figure 3-18. (Left) Initial load frame with load cell to measure force applied. (Right) Wireless node that broadcasts load cell data to computer.

A different load frame was manufactured for further testing of the influence of applied load to the spectra of carbon fiber. The second frame is simpler, with a steel bar in the middle of the frame that can be raised by threaded rods to apply strain to the fiber. The strain is adjusted by using a wrench to turn the

threaded rods forcing the center steel bar up or down. The distance below the steel bar can be measured on each side of the frame using a digital caliper, and applied strain is found using the Pythagorean Theorem. The grips have a much larger contact area to promote more uniform loading of fibers. Additionally index card material paper strips were put on either side of the gripping surface to pad the fiber and prevent slipping.

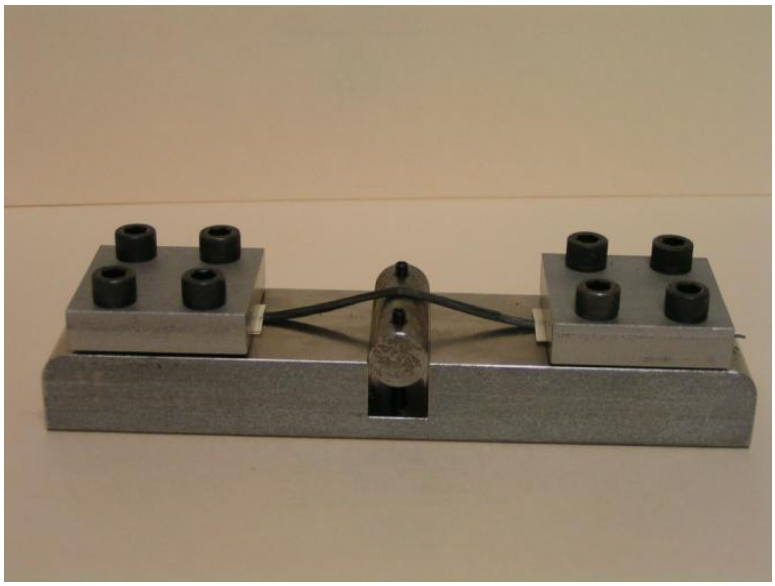

Figure 3-19. Load frame that applies load by raising steel rod in the middle of frame, where applied strain can be calculated using the Pythagorean Theorem. The fibers are oriented parallel to the direction of stretching.

For the testing of Raman spectra changes due to applied strain, fibers are gripped in the load frame (Figure 3-19) and multiple measurements are taken at each strain. Fibers are strained within their elastic range or until they fail. Measurements are also taken of failed fibers. The primary objective in this strain testing is to find correlation between applied strain and Raman band wave-number location. Additionally, samples from failed tanks could be forensically

analyzed to find their stress state at the time of failure. Comparison of the spectrum produced by the failed tank and that of a virgin tank could be made by looking at peak locations, and correlating that to calibrated stress/strain-peak location information.

4 RESULTS

4.1 Spectra of Carbon Fibers and Composites

4.1.1 Carbon Fibers

Although carbon fibers are typically used as part of a composite material, it is necessary to investigate the spectra of the carbon fibers by themselves. The spectra produced by solely carbon fibers are more manageable to investigate because there are less Raman bands due to the less complex material composition. Additionally, spectra produced by just the carbon fiber can allow for deeper analysis of Raman carbon bands shifts with applied strain. Raman spectra of the carbon fibers listed in Section 3.2.1 were tested using a variety of incident lasers and measurement settings.

The pitch-based fibers CN60, CN80, CN90, and YS-95A from Nippon Graphite Fibers spectra are shown in Figure 4-1 using a 752nm incident laser. The response clearly shows the Raman D, G, D', and G' bands as discussed in previous literature, and these particular fibers have very sharp Raman bands as a result of their high level of graphitization during production. The hump that appears in the spectra in the 1700-2500 cm^{-1} range is prevalent in all data collected on the Raman system using the 752 nm laser. It is hypothesized that this is an experimental artifact and could be a factor of optical alignment or other

conditions that exist in the system. The system has since been serviced due to a leak in the water cooling system that could have affected results. It should be noted that even with this experimental artifact, the Raman bands were found to be sharp and to occur precisely where previous literature indicated. Also of note is the measurement of a higher G-band relative intensity than that of the D-band. This can be attributed to the fact that the Nippon Graphite Fibers are highly structured (crystallized) and this relates to the G-band as discussed in the literature review.

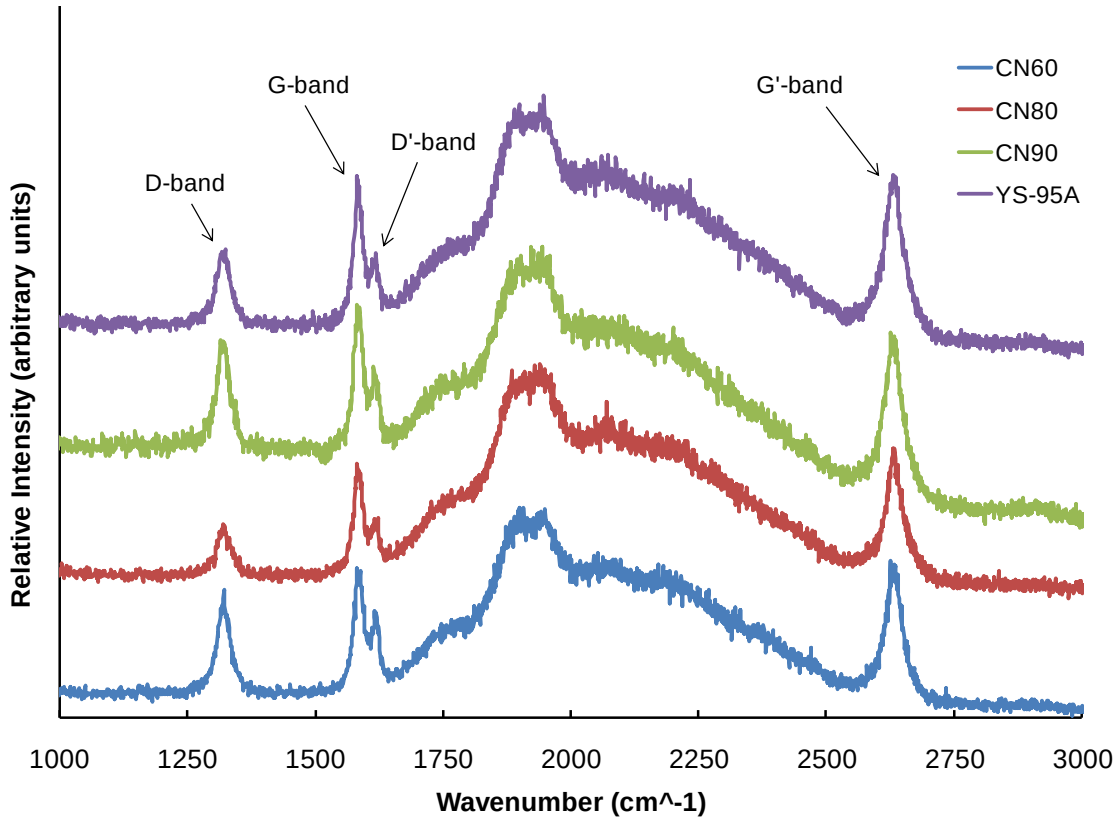

Figure 4-1. Spectra of Nippon Graphite fibers (pitch-based) and identification of the active Raman bands using a 752nm incident laser.

The graphite fibers were also measured using a 514nm incident laser and this is shown in Figure 4-2. It can be seen that the large hump in the 1700-2500 cm^{-1} range is not present. All the Raman bands identified in the 752nm spectra are clearly present in the 514nm spectra.

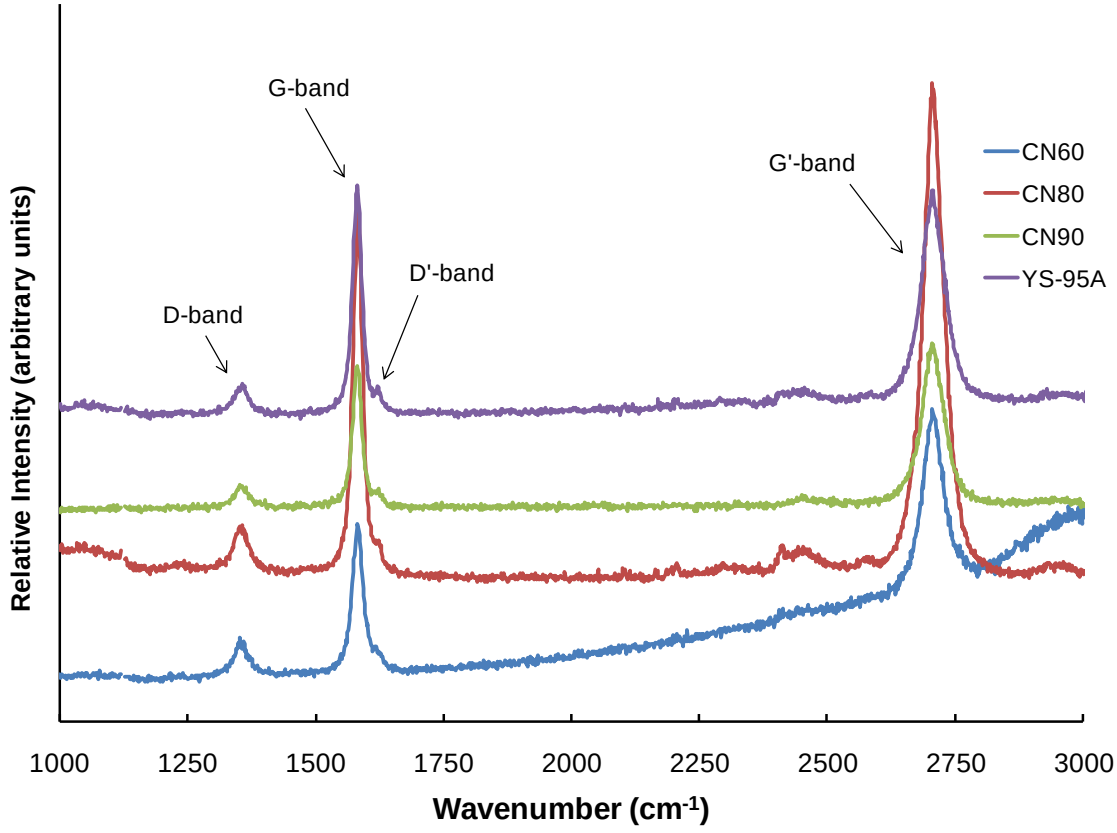

Figure 4-2. Spectra of Nippon Graphite fibers (pitch-based) and identification of the active Raman bands using a 514nm incident laser.

The PAN-based Toray fiber T700 spectra at three different incident laser wavelengths are shown in Figure 4-3. Both the D and G-bands of the fiber are distinctively present. It should be noted that the relative intensity of the D-band and G-band for the T700 fiber is nearly similar. This can be explained by the presence of both ordered and disordered carbon in the material. This differs

from the previous mentioned (Nippon Graphite Fibers) samples that had a much higher intensity G-band from their higher percentage of ordered carbon in the material.

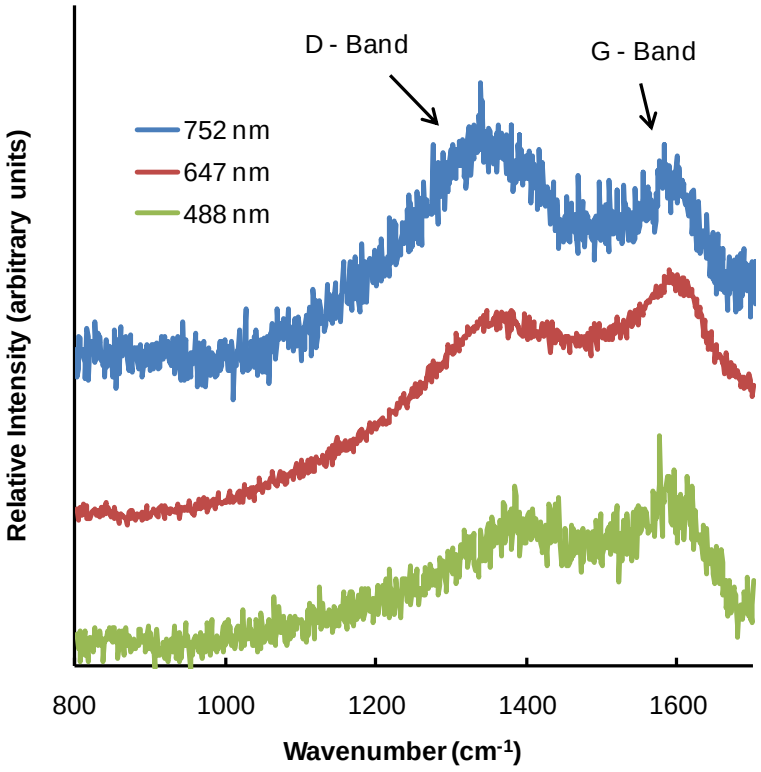

Figure 4-3. Spectra of Toray T700 fiber (PAN-based) and identification of the active Raman bands using incident lasers of 488, 647, and 752 nm.

Figure 4-4 shows spectra of Toray T1000 fiber at both 752 and 514 nm incident laser wavelengths. Due to longer accumulation times during measurement, the spectra of the T1000 produced is much cleaner (higher signal-to-noise-ratio) than the spectra acquired of the T700 fiber. Also of note, are the various smaller peaks in the 514 nm spectra in the region between 2200 and 2800 cm^{-1}. Unlike the closed sample container for the 488, 647, and 752 nm

interchangeable Raman system, the samples under the 514 nm system are exposed to natural light from the room. These smaller peaks can be attributed to the presence of natural light.

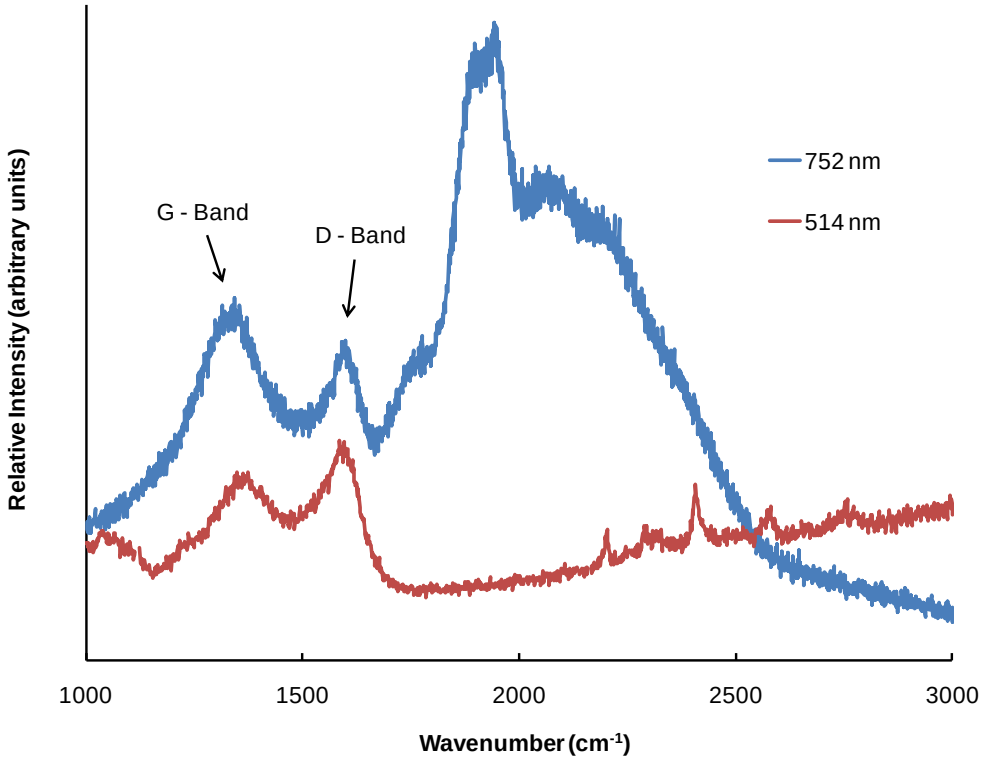

Figure 4-4. Spectra of Toray T1000 fiber (PAN-based) and identification of the active Raman bands using incident lasers of 514 and 752 nm.

The last carbon fiber measurement reported is from Cytec T300 fiber (PAN-based) at 752nm incident laser and is shown in Figure 4-5. The spectrum exhibits both the carbon Raman bands and the experimental artifact present in the other 752 nm measurements.

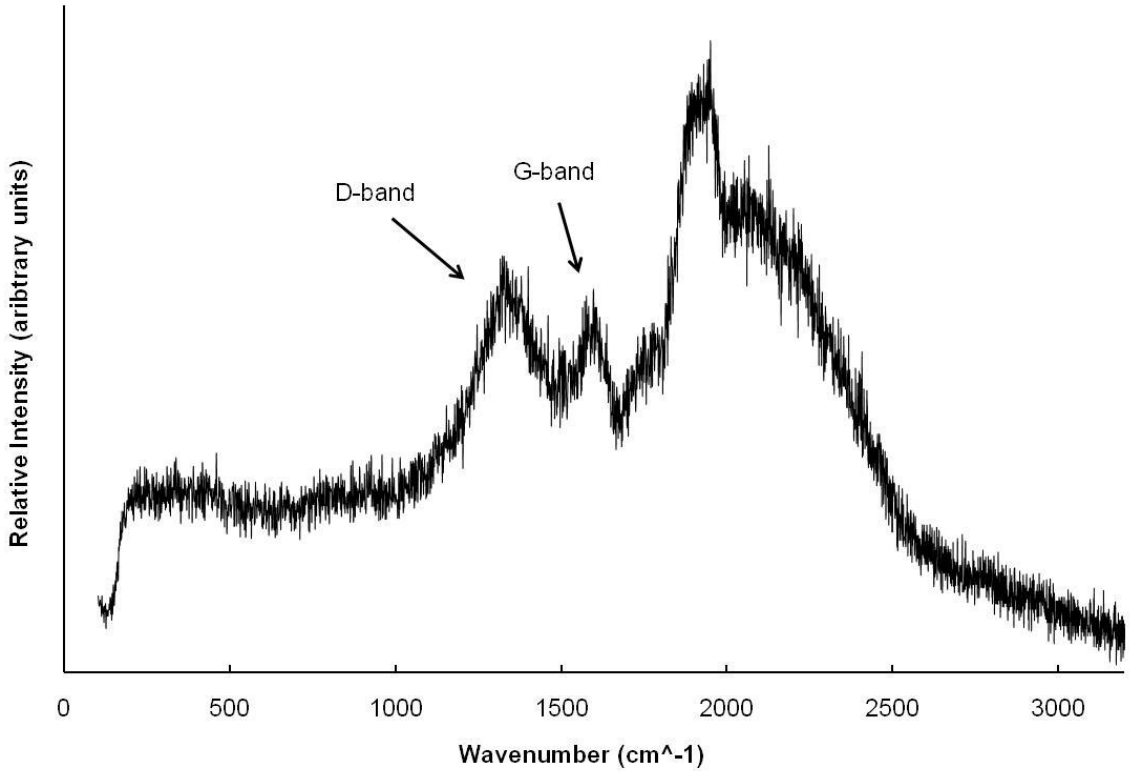

Figure 4-5. Spectra of Cytec T300 fiber (PAN-based) and identification of the active Raman bands using a 752 nm incident laser.

4.1.2 Fiber/Epoxy Composites

Measurement of fiber/epoxy composite material proves to be more difficult because of the more complex nature of the composite material. Both the fibers and the epoxy are highly reflective and affect the ability to clearly focus on a fiber making acquisition of clean spectra difficult. For the pitch-based fibers strand was made using the fiber and Devcon® quick epoxy. The spectra produced contain many more peaks that can be attributed to the material composition of the epoxy as shown in Figure 4-6. Also the surface of a treated fiber likely responds differently than the surface of raw carbon fibers. Comparison of the

raw fiber spectra to the spectra produced by a fiber/epoxy composite is shown in Figure 4-7.

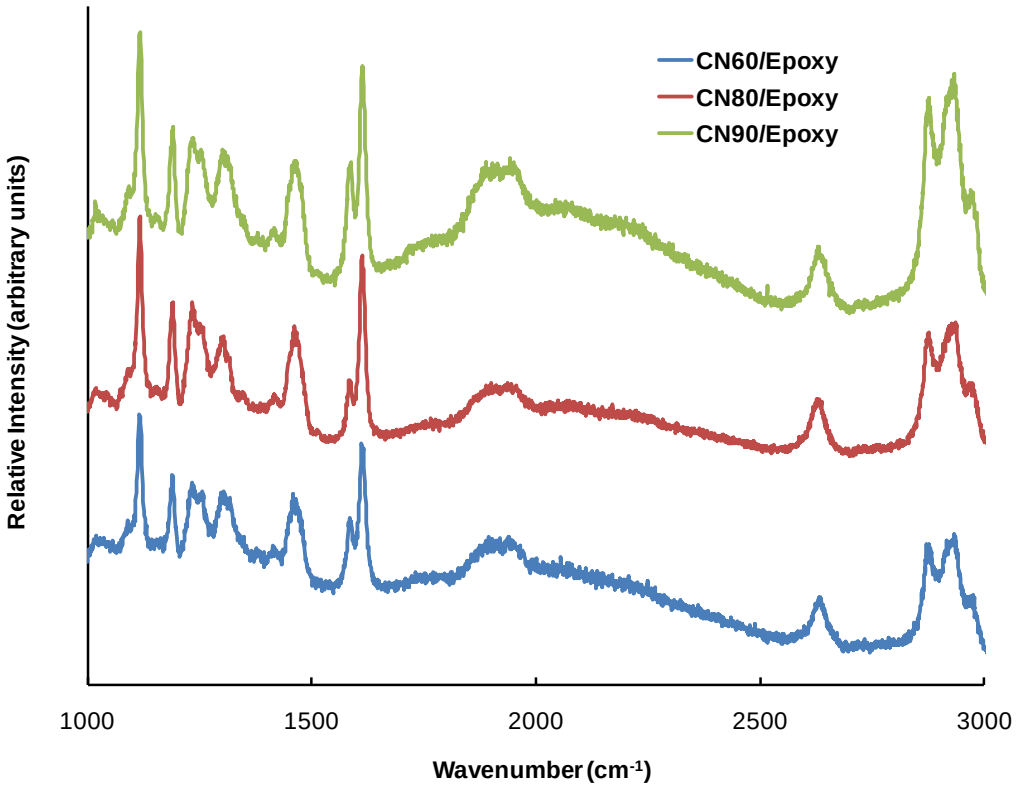

Figure 4-6. Spectra of Nippon Graphite Fibers/Epoxy strand using a 752nm incident laser.

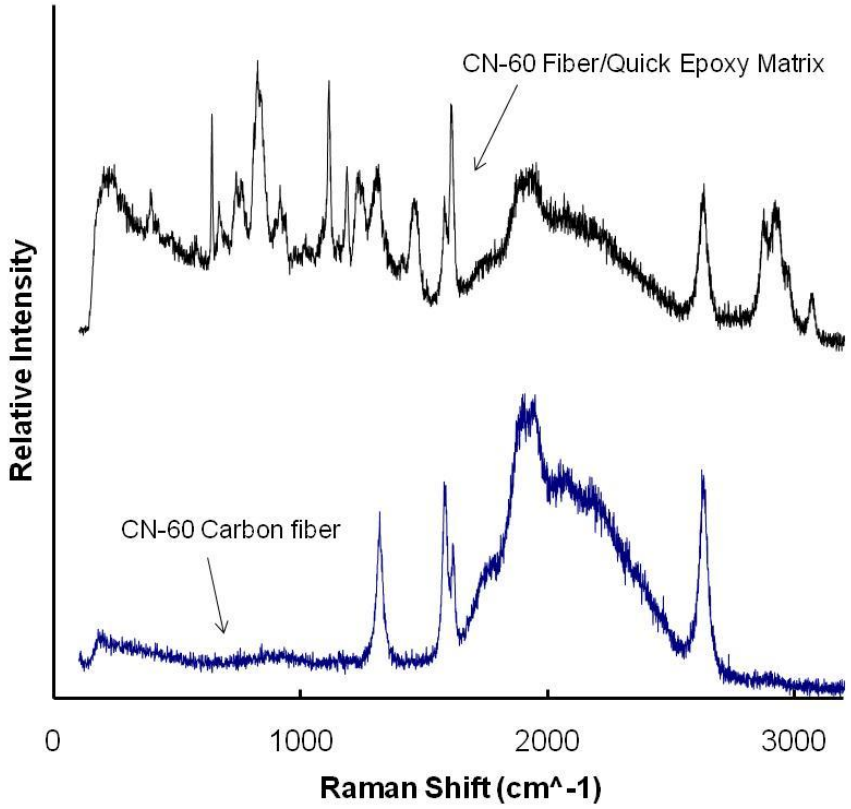

Figure 4-7. Raman spectra of CN-60 Nippon Graphite fiber and CN-60/Quick Epoxy Matrix using a 752nm incident laser.

4.1.3 Spectral Processing and Comparison

To analyze the spectra produced from the carbon fiber, commercial software PeakFit® was used. This peak processing software is important to assist in finding exact peak locations of the Raman bands and other critical peak and overall spectral characteristics. The software enables the user to shape functions to the peaks produced by the spectra and remove or filter errant data from the spectra. For most peaks, deconvolution with a quadratic or linear base line and a 95% filter fit to a Lorentzian amplitude was used to focus on only the distinct peaks that relate to the known Raman bands produced. Deconvolution is

a mathematical procedure that is often used to remove smearing or broadening of peaks arising due to the imperfections of an instrument measuring system. Figures 4-8 through 4-10 show a typical peak processing procedure in PeakFit®. Statistical information that is calculated during the peak deconvolution process includes peak location, peak intensity, and full-width-at-half-maximum (FWHM) values. Relative changes to Raman data also may yield important information for condition assessment of a material.

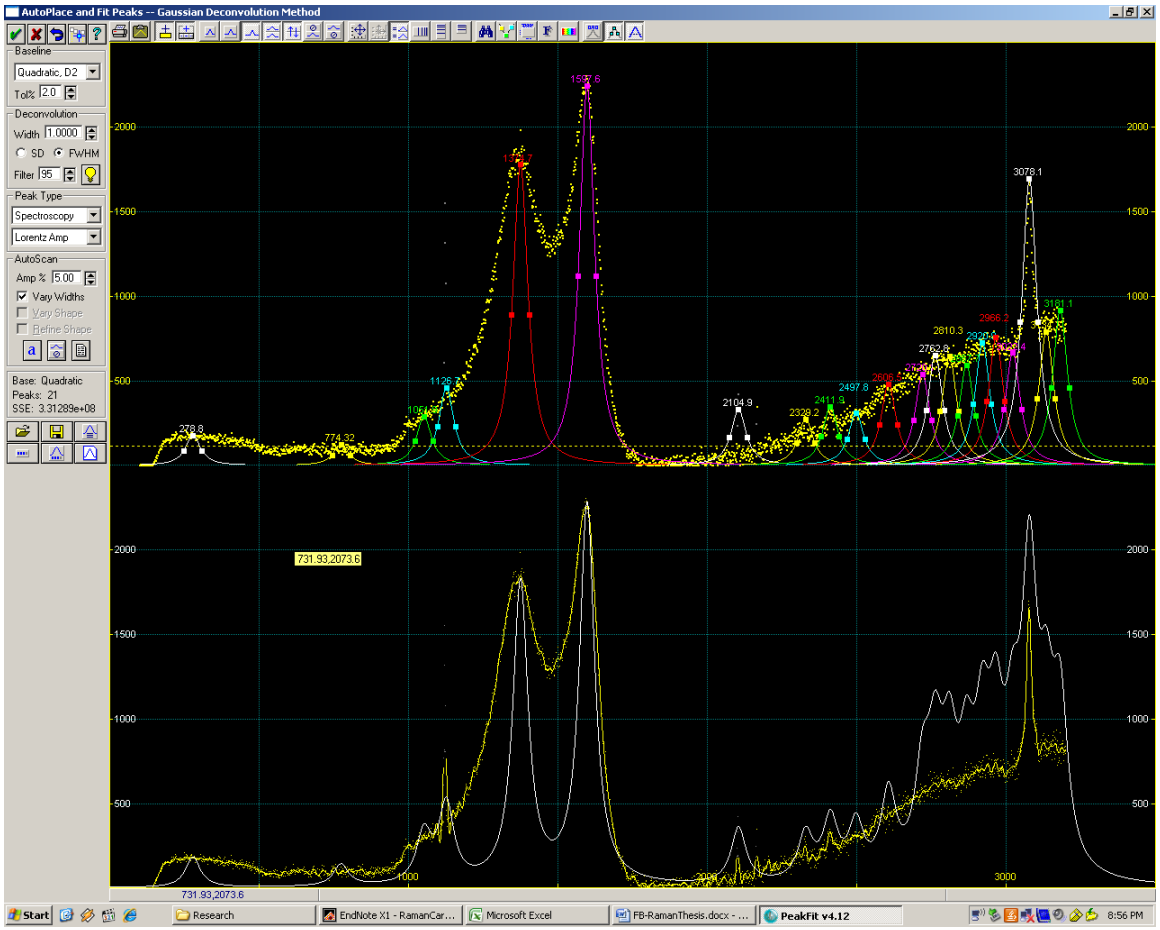

Figure 4-8. T1000 fiber spectrum from a 514nm incident laser. PeakFit® allows users to select filters and specifications to remove false peaks that may appear due to sampling imperfections.

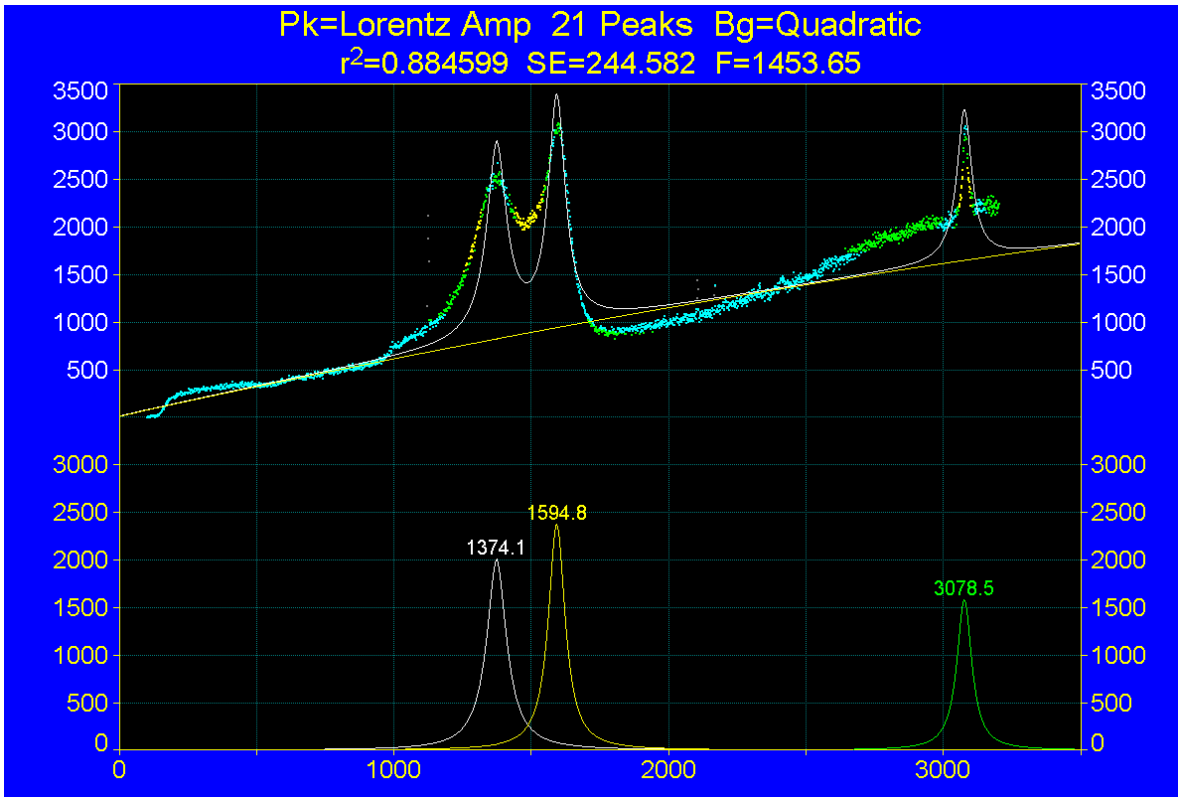

Figure 4-9. Spectrum after deconvolution and errant peak removal.

Peak Summary

File Edit Style Options

Description: C:\Documents and Settings\fdbq36\Desktop\Research\Raman Data\09-02-26 - MU EE (T

File Source: c:\documents and settings\fdbq36\desktop\research\raman data\09-02-26 - mu ee (t1000)\data\09-02-16\t1000_8.txt

Measured Values

Peak	Type	Amplitude	Center	FWHM	Asym50	FW Base	Asym10
1	Lorentz Amp	2015.97585	1374.14706	90.8000435	0.99999995	302.666812	0.99999998
2	Lorentz Amp	2377.57020	1594.84416	73.7186997	1.00000026	245.728999	1.00000009
3	Lorentz Amp	1582.62243	3078.50684	65.5138651	0.99999992	218.379550	0.99999997

Peak	Type	Anlytc Area	% Area	Int Area	% Area	Centroid	Moment2
1	Lorentz Amp	2.8754e+05	161.941015	2.82e+05		1379.45671	43586.2620
2	Lorentz Amp	2.7532e+05	155.058825	2.7114e+05		1595.70205	35569.4505
3	Lorentz Amp	1.6287e+05	91.7267517	1.487e+05		3042.42255	33024.6178
	Total	1.7756e+05	100.000000	0.00000000	100.000000		

Figure 4-10. Numerical analysis that PeakFit® provides after processing.

4.1.4 Raman Bands

Detection of Raman bands is the first necessary step for Raman spectral analysis of carbon fiber and carbon fiber composites. Table 4-1 summarizes the detected Raman bands for each material at each incident laser wavelength and compares them to peaks from literature. These detected bands are also discussed in further detail in the literature review. The primary D and G bands are of specific focus as they relate to the molecular vibrations of the disordered and ordered carbon respectively, and are present in all the material tested, providing the best opportunities for comparison of spectra. The listed values in Table 4-1 are based on average peak location values of each material with no applied strain.

Table 4-1. Raman peaks of from literature and how they correspond to average peaks found during measurements of raw carbon fibers at 752 nm.

	Raman Band Locations (cm^{-1})					
From Literature	~1330	~1585	~1613	~2630	~2720	~2950
Pitch-based @ 752nm						
Nippon CN-60	1321	1586	1617	2628	-	-
Nippon CN-80	1323	1584	1618	2631	-	-
Nippon CN-90	1319	1582	1615	2628	-	-
Nippon YS-95A	1322	1584	1615	2633	-	-
PAN-based @ 752nm						
Toray T700	1345	1595	-	-	-	-
Toray T1000	1341	1596	-	-	-	-
Cytec T300	1335	1597	-	-	-	-

4.2 Strain Testing Results

4.2.1 Peak Shift

The specific peak location can be examined for each spectrum based on statistical analysis from PeakFit® as described in the spectral processing section. It is found that for some types of fiber and also documented in previous literature that peak locations for a given Raman band decrease as a function of increased applied strain. The pitch-based fibers did not exhibit this peak shift when undergoing strain testing. One reason for the pitch-fibers not exhibiting a peak shift is that the pitch-fibers tested are much stiffer (higher modulus) than the PAN-based fibers tested. This stiffness decreases the possible elongation and elastic range of the fibers making testing strain within the elastic range very difficult. For the PAN fibers tested, Toray T1000 fiber exhibited the most consistent peak shift as strain was applied to the fibers. Examples of Raman peak shift of the T1000 fiber using a 752 nm and 514 nm incident laser wavelength are shown in Figures 4-11 and 4-12 respectively. From large amounts of data collected during strain testing, relationships have been developed for peak shift as a function of applied stress. These relationships are shown in Figures 4-13 thru 4-16 for the both the D and G Raman bands at 752 nm and 514 nm incident laser. The T1000 had the most consistent and observable peak shift of the fibers tested. This can be attributed to the high stiffness of this fiber type when comparing it to other PAN-based fibers. For the T1000 fiber the peaks appear to shift at least 5 wavenumbers / percent applied strain. In some instances and in some other literature this shift is higher. Due to

the gripping mechanism on the load frame it is difficult to be certain that all the fibers are under the exact same amount of applied strain. This could account for the variance in the peak location results as different locations on the fiber sample are under different levels of strain changing their vibrational modes of interaction that dictate the Raman response. Additionally, results of the peak shift of Toray T700 fiber during strain testing using a 752nm laser are shown in Figures 4-17 and 4-18. The peak shift of the T700 fiber is not as distinct as the T1000 fiber because of the lower performance characteristics. Generally, the higher the stiffness of the fiber the more distinct and strain sensitive the fibers Raman bands produced will be.

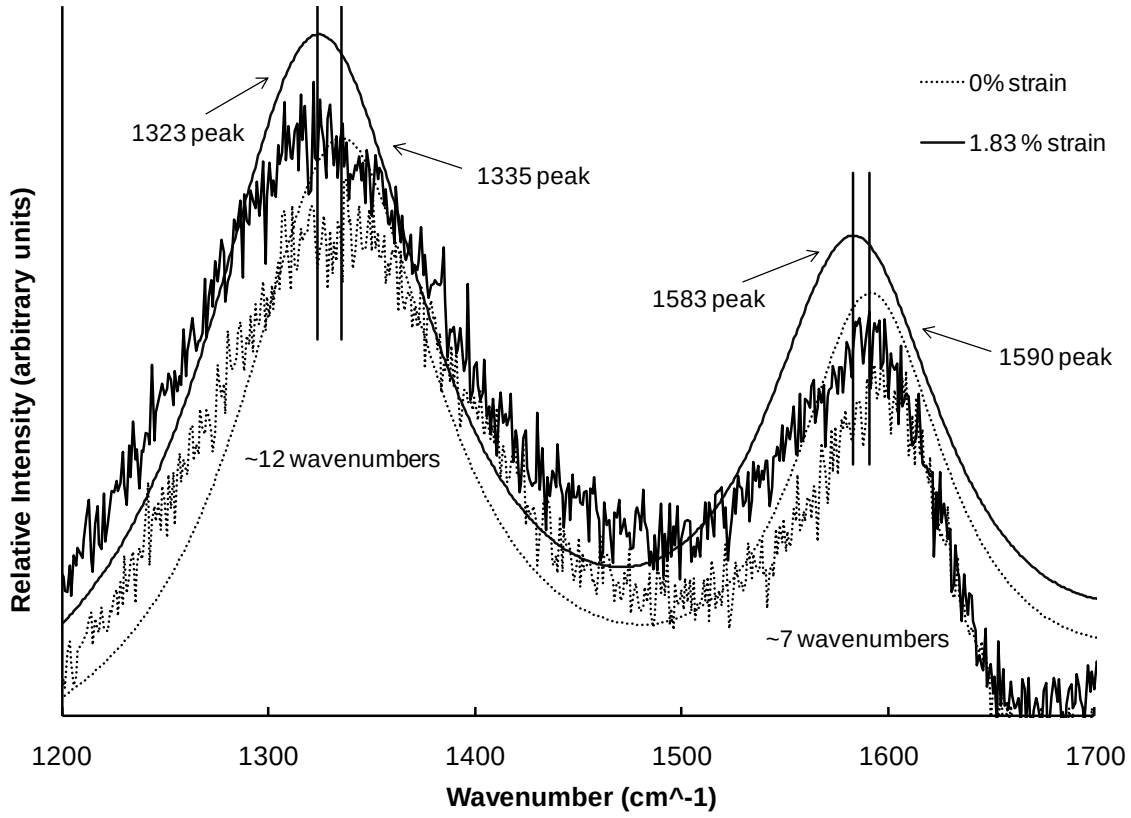

Figure 4-11. Zoom-in of a raw and processed spectra of T1000 carbon fiber showing D and G band shifts at 0% and 1.83% applied strain using a 752nm incident laser.

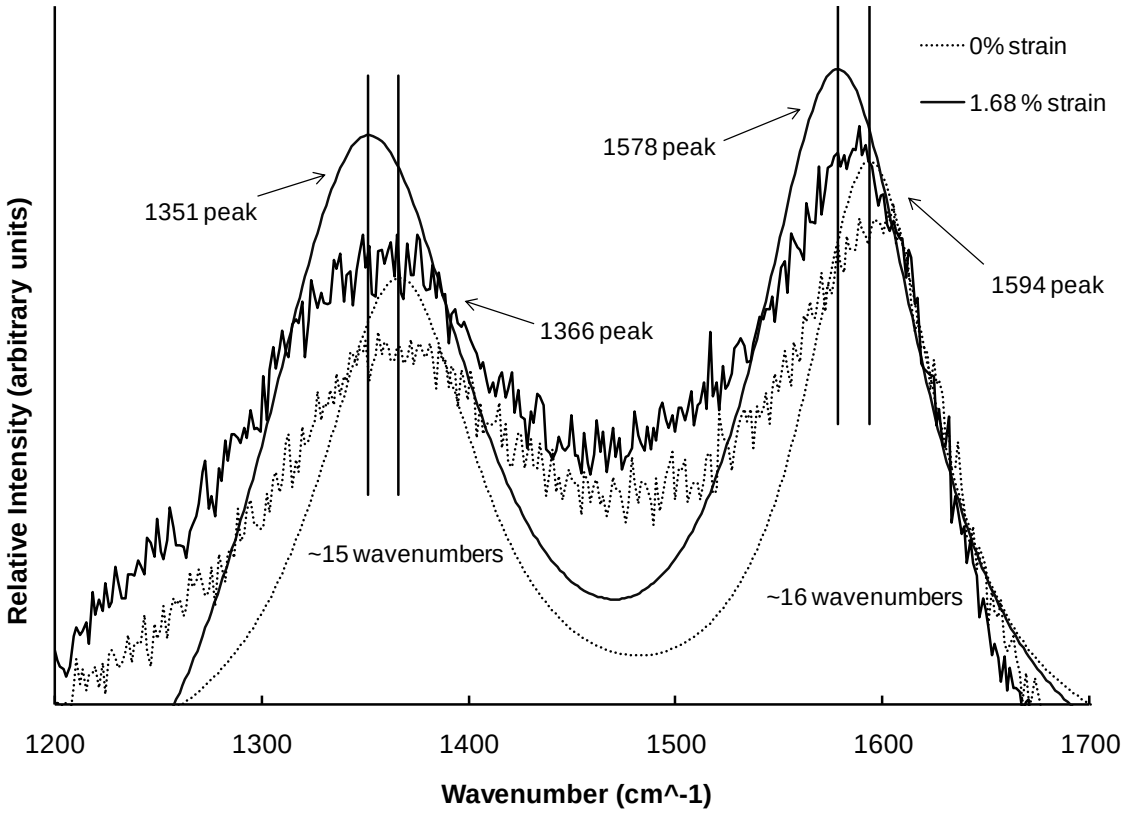

Figure 4-12. Zoom-in of a raw and processed spectra of T1000 carbon fiber showing D and G band shifts at 0% and 1.68% applied strain using a 514nm incident laser.

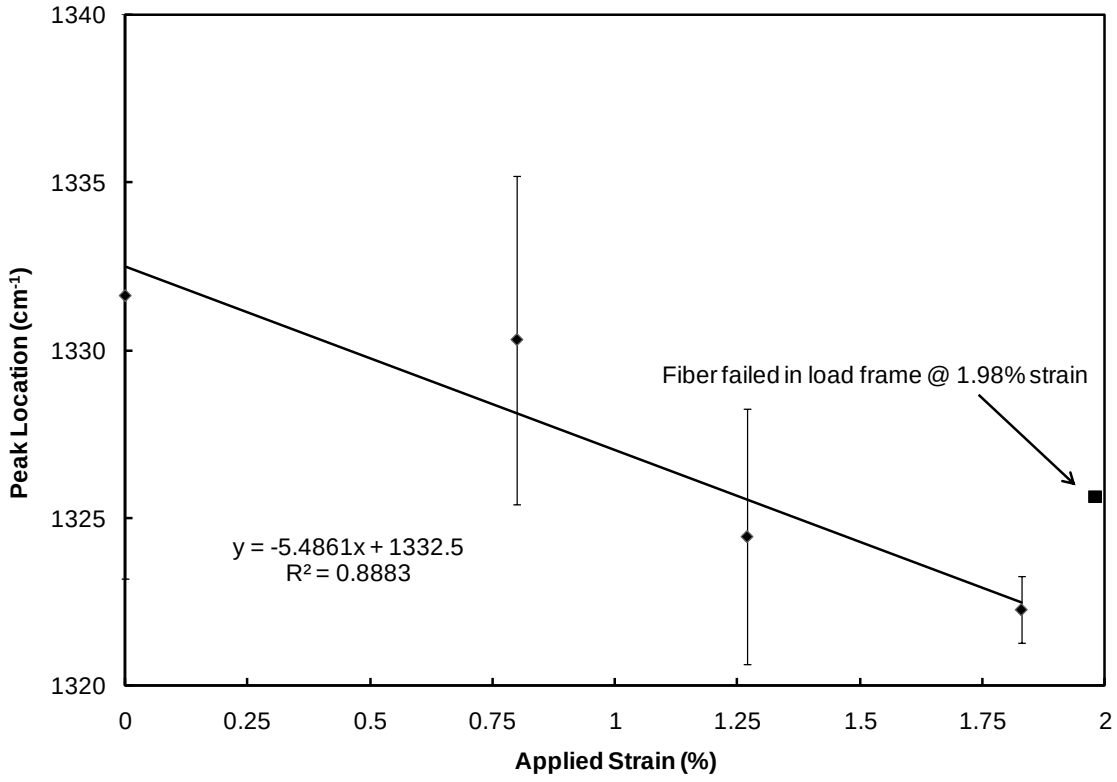

Figure 4-13. Peak shift of 1330 cm^{-1} peak for T1000 fiber using a 752 nm incident laser. Each value is an average of 3 measurements, except for the last data point which is singular.

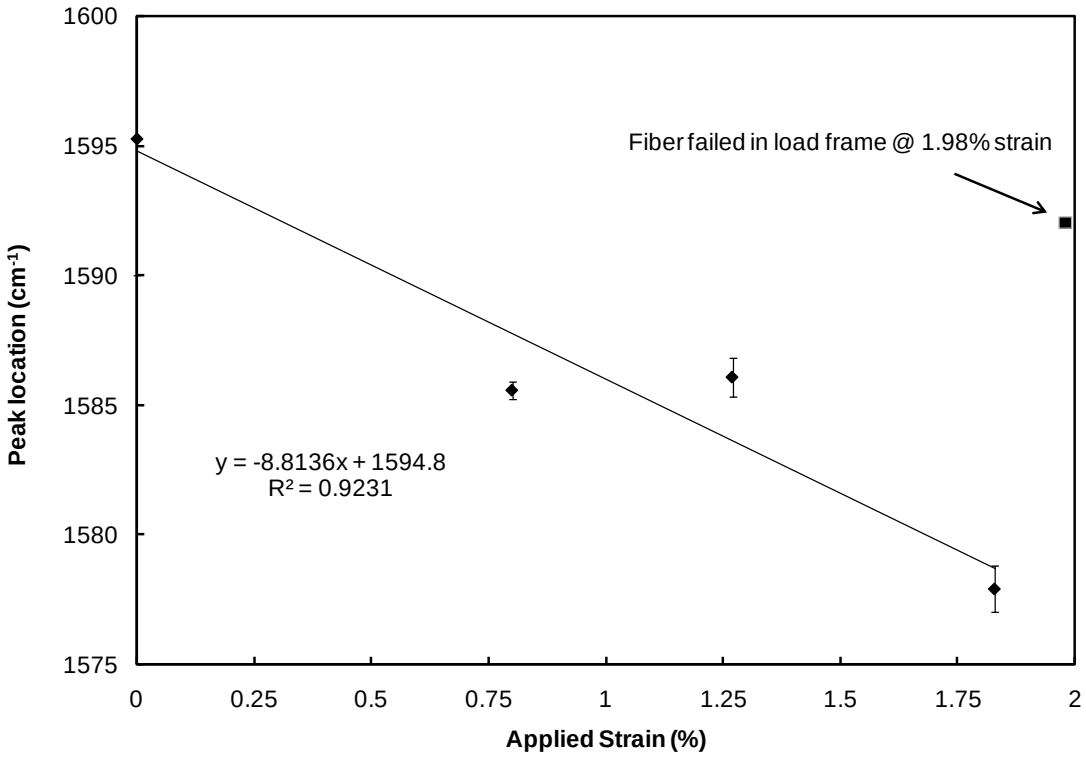

Figure 4-14. Peak shift of 1585 cm^{-1} peak for T1000 fiber using a 752 nm incident laser. Each value is an average of 3 measurements, except for the last data point which is singular.

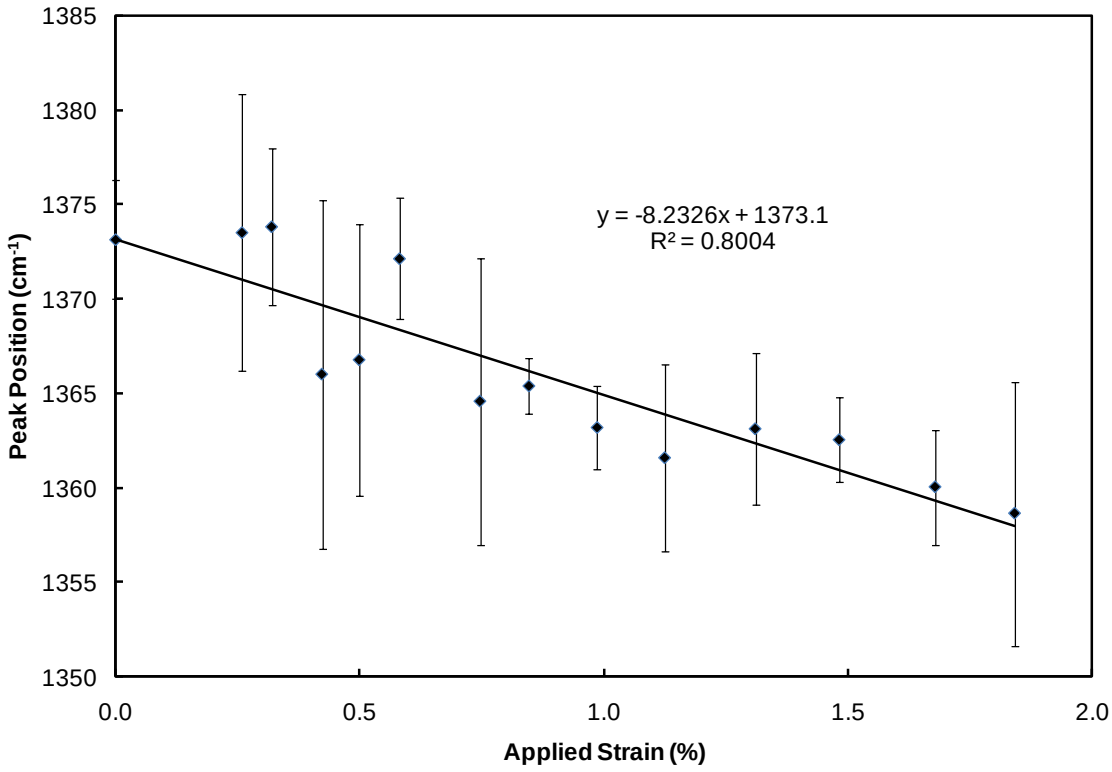

Figure 4-15. Peak shift of 1360 cm^{-1} peak for T1000 fiber using a 514 nm incident laser. Each value is an average of 4 measurements.

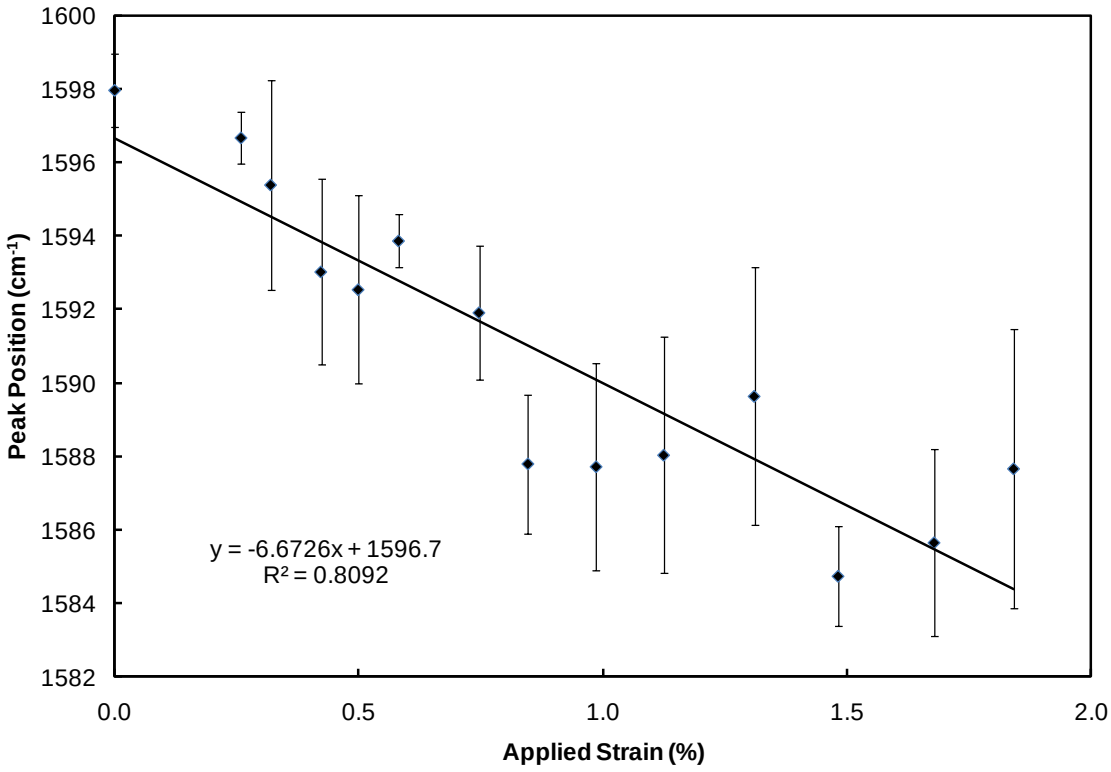

Figure 4-16. Peak shift of 1585 cm^{-1} peak for T1000 fiber using a 514 nm incident laser. Each value is an average of 4 measurements.

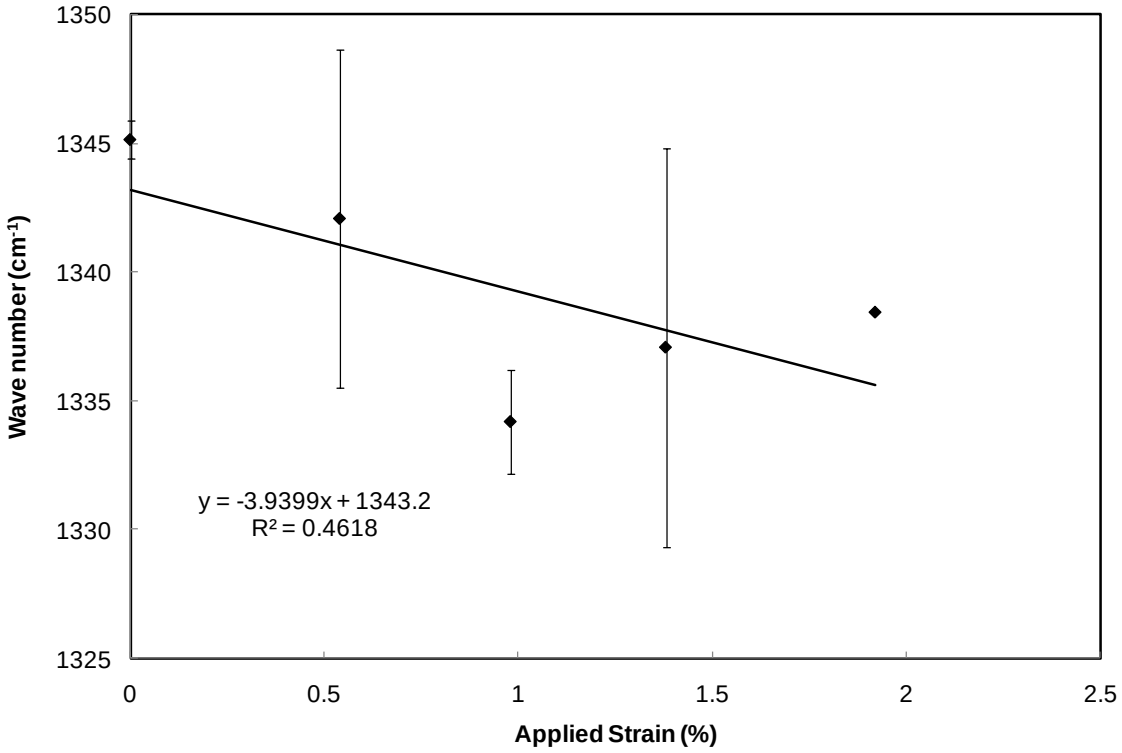

Figure 4-17. Peak shift of 1340 cm^{-1} peak for T700 fiber using a 752 nm incident laser. Each measurement is based off an average of 3 values, except for the last data point which is singular.

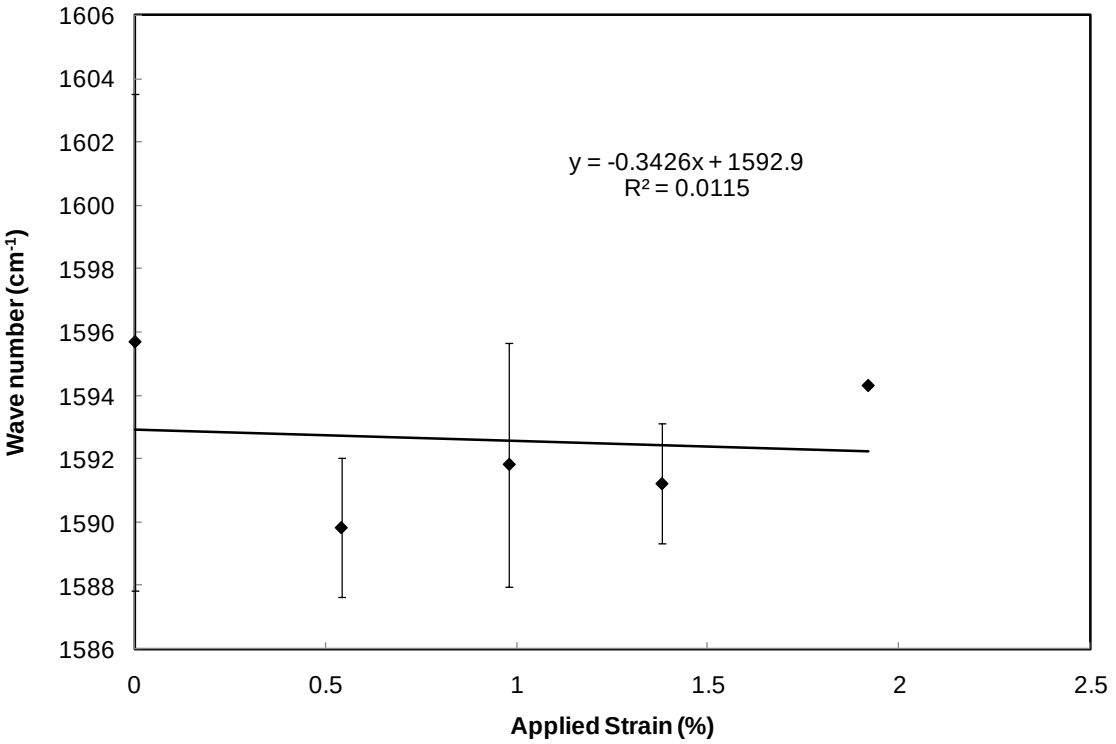

Figure 4-18. Peak shift of 1590 cm^{-1} peak for T700 fiber using a 752 nm incident laser. Each measurement is based off an average of 3 values, except for the last data point which is singular.

Strain testing was also conducted on the T-40 composite strand ripped from a tank sent from NASA. As previously mentioned in the experimental section this material is typical of wrapping in COPVs that NASA uses for gas storage on shuttles. Testing the composite materials is more difficult due to the additional material present making focusing on fibers more difficult and a higher variance in the results. The stiffness of the material is also much greater, but in theory the fibers should work as more of a system due to the addition of epoxy/fiber composite interaction and be more likely to be under the same

applied strain in multiple locations leading to more consistent values. More extensive strain testing of all fiber and composite types would be useful to develop more dependable relationships on peak location v. applied strain.

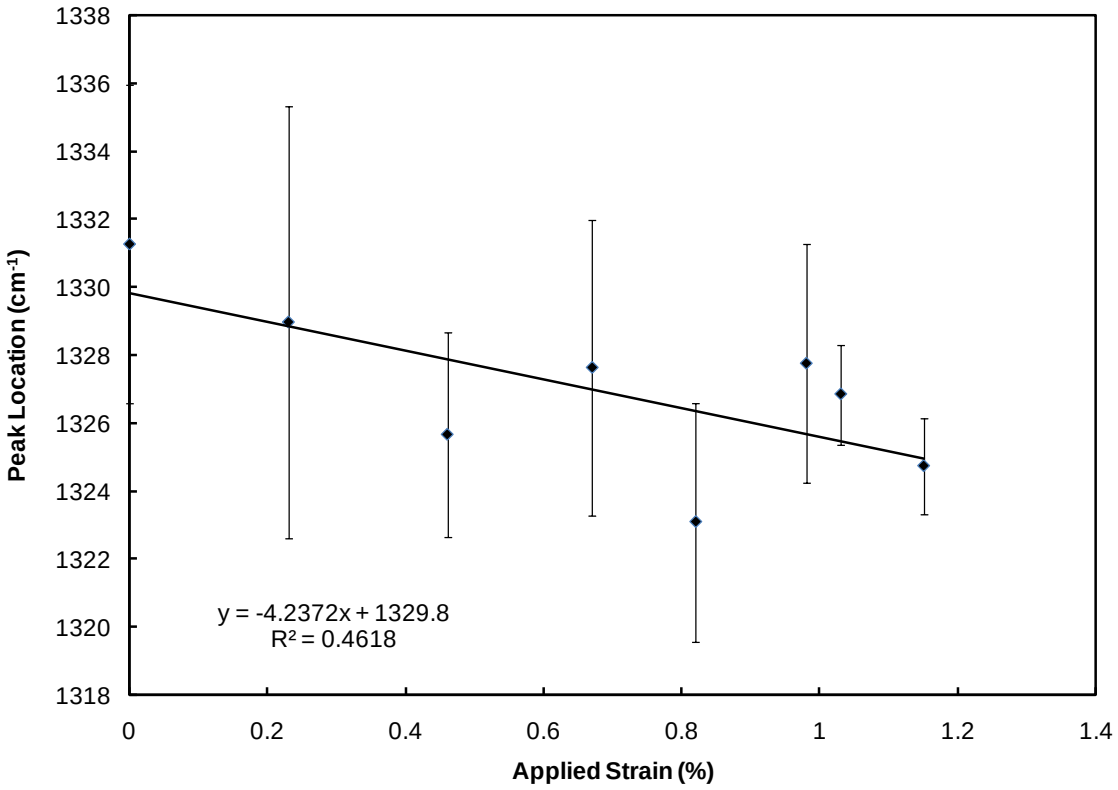

Figure 4-19. Peak shift of 1330 cm^{-1} peak for T-40 strand using a 752 nm incident laser. Each value is an average of 3 measurements.

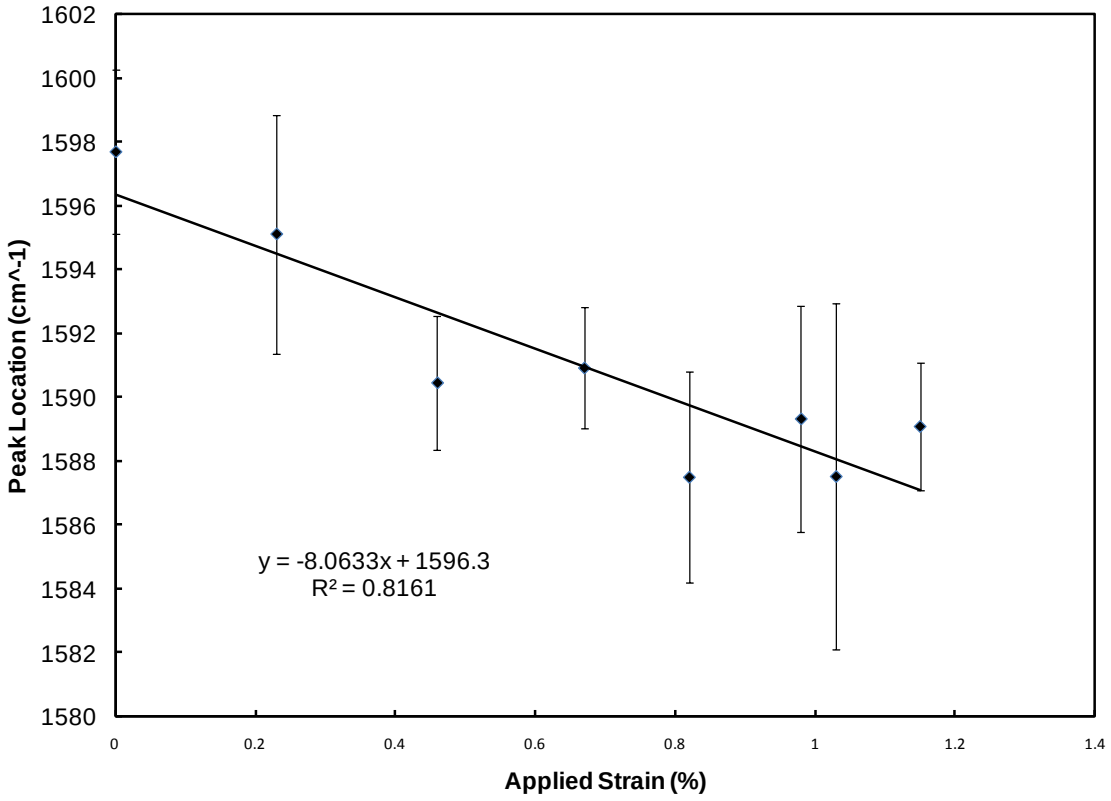

Figure 4-20. Peak shift of 1590 cm^{-1} peak for T-40 strand using a 752 nm incident laser. Each value is an average of 3 measurements.

4.2.2 Full-width-at-half-maximum

Besides peak location, other comparisons must be able to be made between different acquired spectra. One such geometric value is the Full-width-at-half-maximum value (FWHM). This value is a numerical value relating to the width at half the maximum value of each peak. As part of the deconvolution of peaks, Peak-Fit calculates the FWHM of each peak. In order to understand how this value is useful it is necessary to normalize this using one of the peaks as a reference. This is done by establishing a ratio of FWHM of each peak compared to FWHM of a reference peak. For analysis the reference peak chosen was that

of the D-band that is present between 1330 and 1360 cm^{-1} and can be detected in all material tested.

Figures 4-21 and 4-22 show the FWHM ratio of the T1000 fiber samples using 752 and 514nm incident lasers respectively. From these figures it can be seen that generally as the applied strain increases, the FWHM ratio of the G-band relative to the D-band decreases in value. Of note is the failed fiber that produced nearly the same result as the fiber with 0% strain in Figure 4-21. This is to be expected as the measurement of the failed fiber should be similar to that of fibers with no strain since the fibers have failed at the point of stress concentration leaving the rest of the fibers to go back to their relaxed state at 0% applied strain. Theoretically the fibers should not undergo damage at a molecular level if they have amounts of strain applied only within their elastic region.

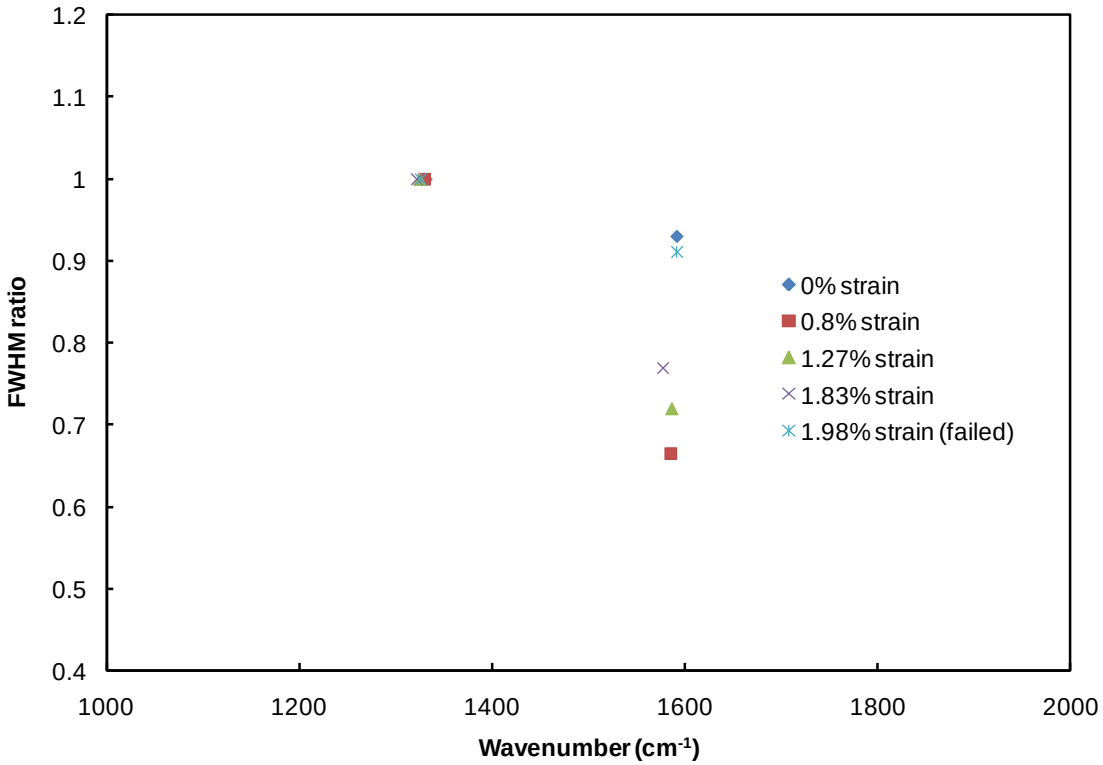

Figure 4-21. FWHM ratios of T1000 fiber at different applied strains using a 752nm incident laser. Each point is based on an average of several values.

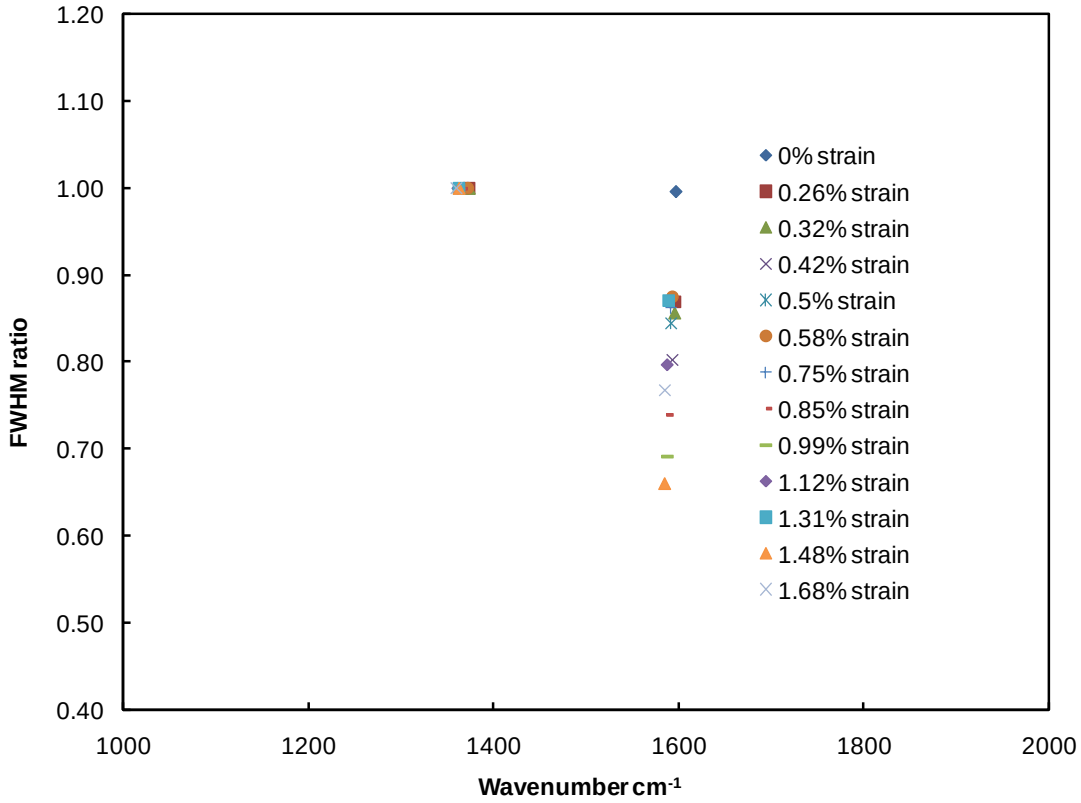

Figure 4-22. FWHM ratios of T1000 fiber at different applied strains using a 514nm incident laser. Each point is an average of several values.

Figure 4-23 shows the FWHM ratio of composite material T-40/epoxy ripped from a NASA COPV. Unlike the results for the raw T1000 fiber there is not an evident trend in the FWHM ratio as strain is applied. One reason for this can be attributed to the nature of how composite materials act compared to that of individual fibers. With the fibers embedded in an epoxy matrix, load is transferred to the composite system of fibers that act in all directions instead of being applied unidirectional as with the raw fibers. The fiber portion of the composite matrix has fibers going in all directions since the material was used as

a wrapping component of the composite. So as the strain is increased using the load frame the fibers do not act unidirectional in their force distribution.

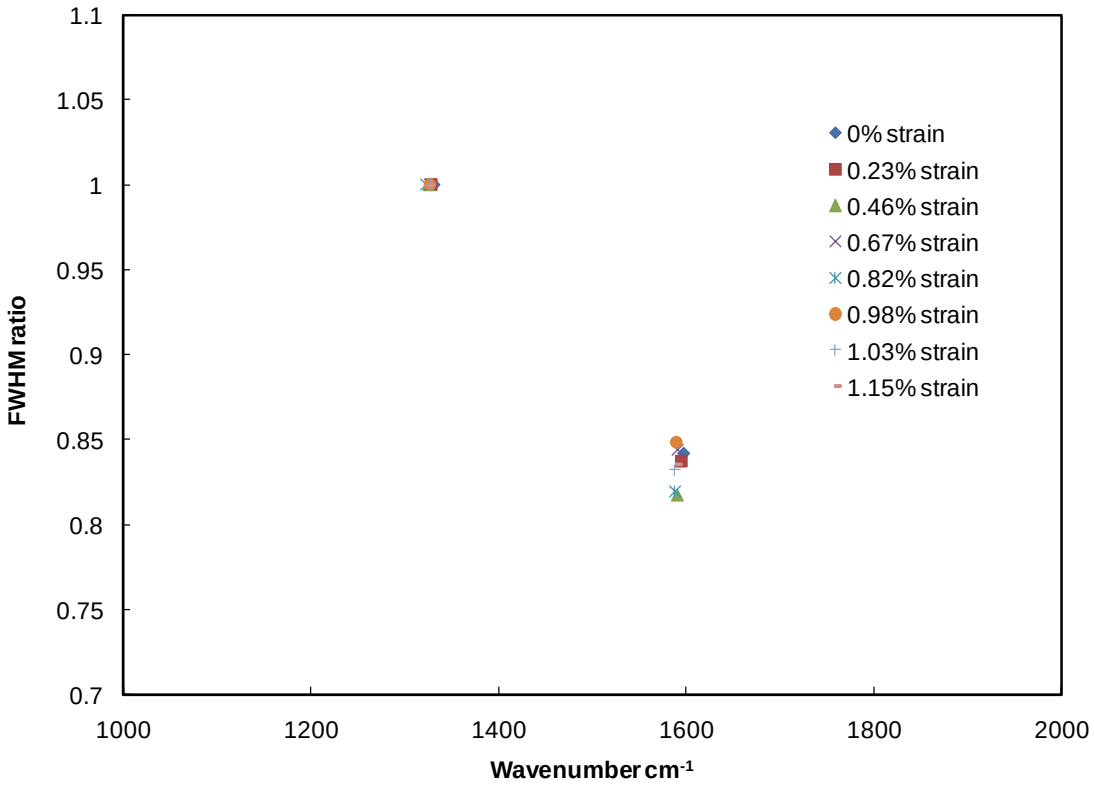

Figure 4-23. FWHM ratios of T-40 strand at different applied strains using a 752nm incident laser. Each point is based on an average of several values.

4.2.3 Intensity

The intensity of spectra produced by Raman instruments can vary greatly due to sampling techniques and material/energy interactions. For intensity analysis of spectra it is necessary to compare of the intensity of peaks relative to a reference peak instead of comparing absolute values of intensity that are essentially arbitrary units anyway. In some cases intensity of a given spectrum can vary by several orders of magnitude even for the same material. Using a

relative intensity approach is also another way to quantify the geometric changes occurring in the spectra produced. For this analysis the intensity ratios were established relative to the D-band associated with disordered forms of carbon.

Figures 4-24 and 4-25 show the intensity ratio at different strain levels for T1000 fiber at both 752 and 514nm. Generally the intensity ratio of the D-band relative to the G-band decreases as the strain increases. The intensity of the D-band is associated with ordered forms of the carbon hexagonal lattice structure. This can be explained since as the fibers are strained the molecular structure will become stressed and failure of carbon-carbon bonds at points within the lattice structure will lead to a higher portion of disordered carbon. Of note is the fact that the intensity ratios of the D-band relative to the G-band using the 514nm incident laser are much higher than that of the 752nm laser. As stated before, the intensity of a spectrum is not nearly as important or informative as the relative changes that occur within it. The data for the 514nm and 752nm incident lasers was collected using a different optic system with separate calibrations and operating conditions. Despite the different specific value of ratios, the trend for both incident lasers is the same with a decreasing G-band intensity as strain level increases.

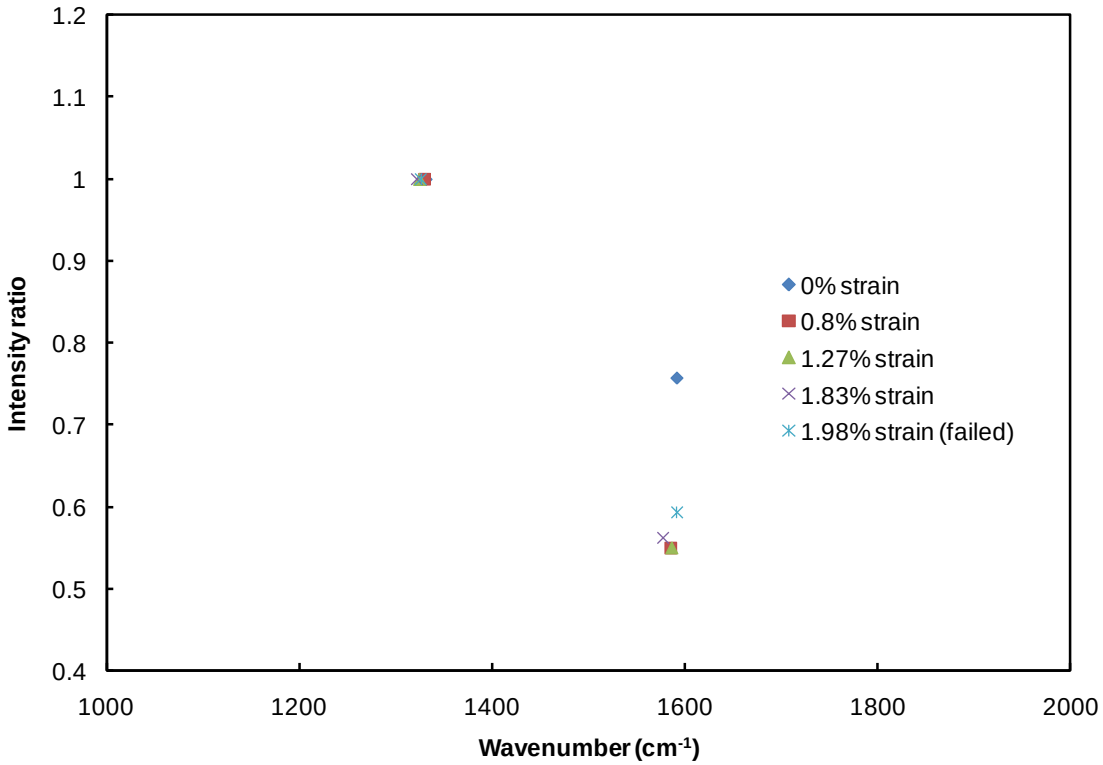

Figure 4-24. Intensity ratios of T1000 fiber at different applied strains using a 752nm incident laser. Each point is based on an average of several values.

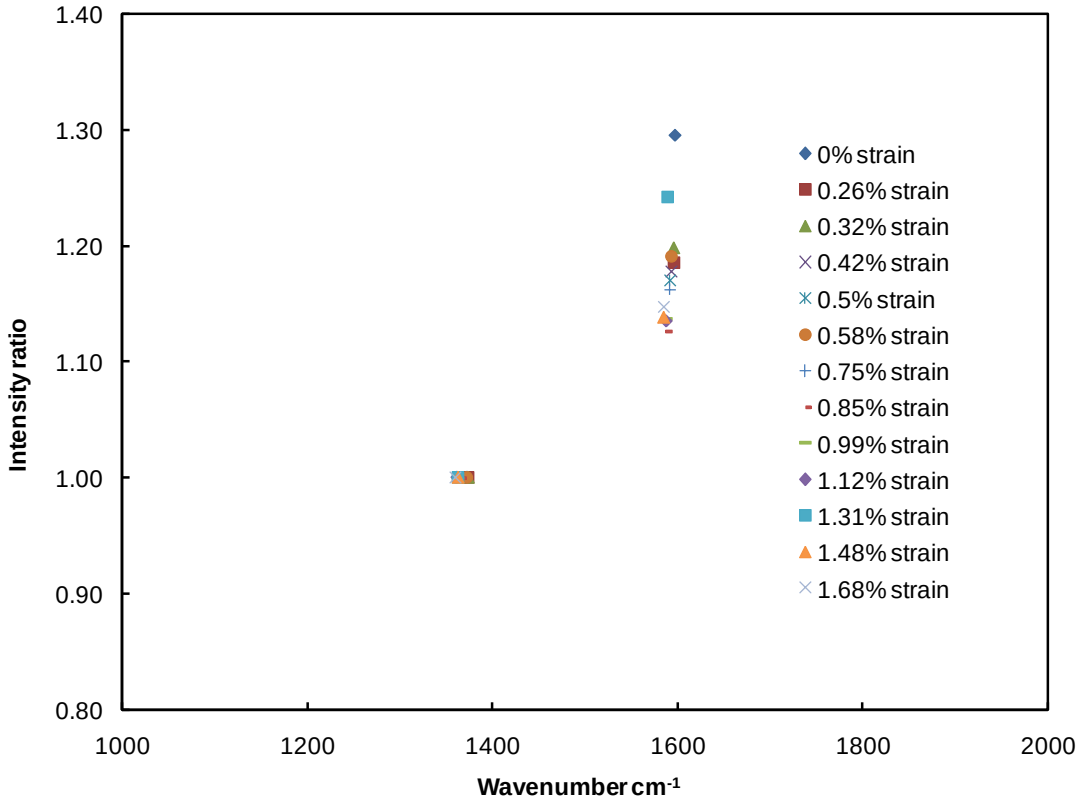

Figure 4-25. Intensity ratios of T1000 fiber at different applied strains using a 514nm incident laser. Each point is based on an average of several values.

Shown in Figure 4-26 is the intensity ratio of the T-40 strand at different levels of applied strain. As with the raw T1000 fiber the intensity of the D-band relative to the G-band decreases as strain level is increased. This result is important because it shows that the relative intensity changes of the composite material follow roughly the same pattern as that of the raw fiber. Ideally the results of the composite material should yield better results with stronger consistency as the material should work as a system and evenly disperse the applied strain throughout the material. A number of problems occur when measuring the composite material. The material is very difficult to focus on from

the outer side because of the reflective nature of the epoxy. Another issue is that the orientation of the fibers are not in-line with the uniaxial applied strain because the fiber portion of the composite material is wrapped in all directions.

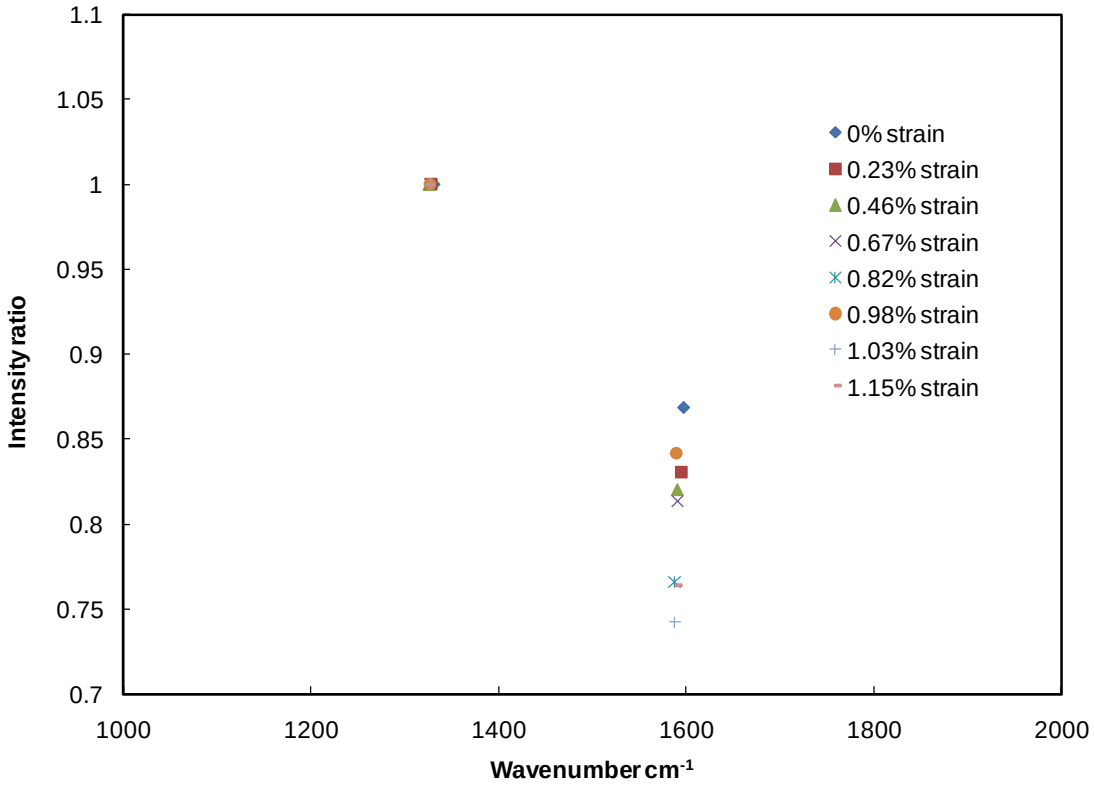

Figure 4-26. Intensity ratios of T-40 strand at different applied strains using a 752nm incident laser. Each point is based on an average of several values.

4.3 Composite Material from Tanks

The composite materials provided from the burst tanks as shown in images in the experimental section have a distinctively different spectrum on the outer and inner sides of the samples. The inner portion of the samples can be focused on an individual carbon fiber due to the exposure of the fiber/epoxy matrix. The outer portion of the samples is difficult to focus on an individual fiber

due to the reflective nature or protective coating on the outside of the tanks. The response from the outside is similar to that of the carbon fiber and epoxy composites discussed in the previous section.

The response of the T-40 sample at 752 nm incident laser is shown in Figure 4-27. It is noted that the inner portion of the sample was focused on a single carbon fiber and resulted in the typical D and G-bands in addition to the large experimental artifact hump present in the other 752 nm results. The outer measurement contains the spectra of the fiber and the epoxy material as well as the artifact between 1700 and 2400 cm^{-1} of the 752 nm system.

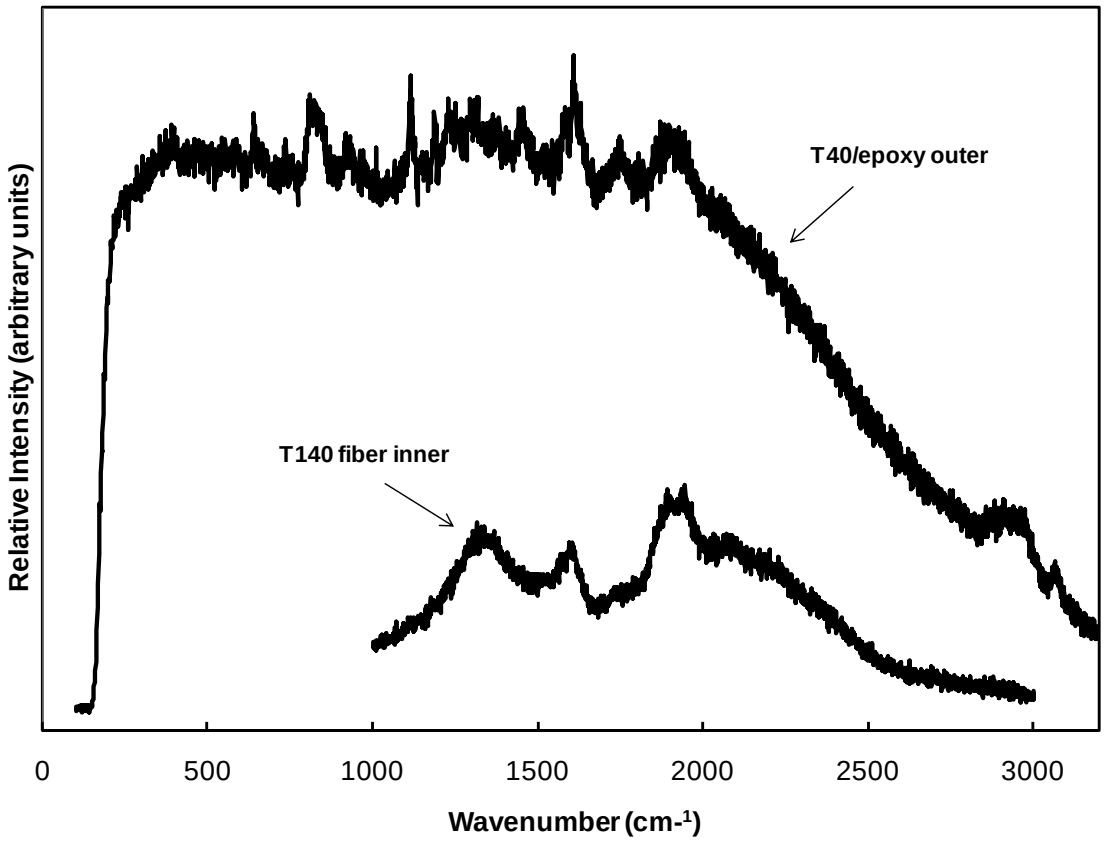

Figure 4-27. Raman spectra of T-40/epoxy ripped strand from a burst tank using a 752 nm incident laser.

The sectioned pieces from the two burst tanks sent to us were tested at 488, 514 and 752 nm incident laser wavelengths. For both laser wavelengths the distinct D and G carbon bands can be identified from measuring the outer or inner portion of the sample. The 488 and 514nm lasers are less sensitive than the 752nm because there is less sample penetration, a function of wavelength. With the shorter wavelength lasers almost all of the light is reflected back with only small amounts penetrating through the coating to find the active Raman bands. For both the T1000/epoxy sample and the IM7/epoxy with peal-ply treatment the outside spectra can be more clearly identified using the results from the 752 nm laser. Figures 4-28 thru 4-33 show the response of the burst tank samples at each wavelength. Further studies on the Raman response of the epoxy materials used would be useful.

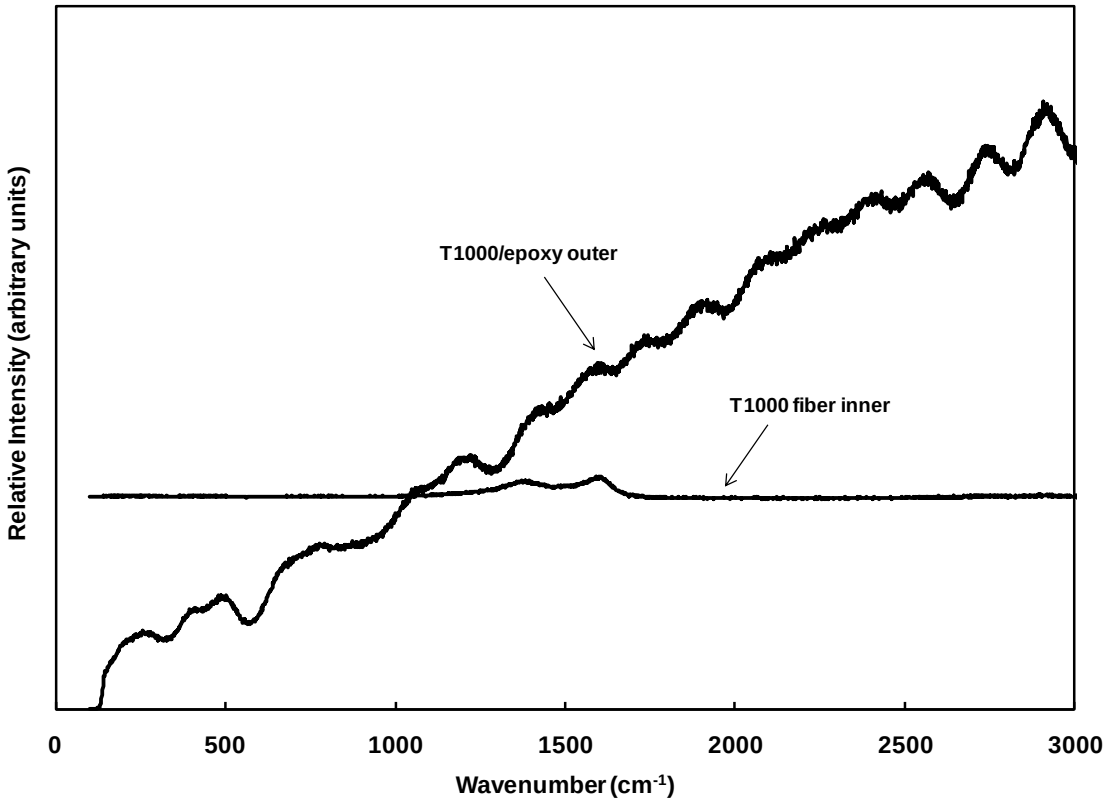

Figure 4-28. Raman spectra of T1000/epoxy burst tank samples showing measurements of the inner and outer portions of the tank using a 488 nm incident laser.

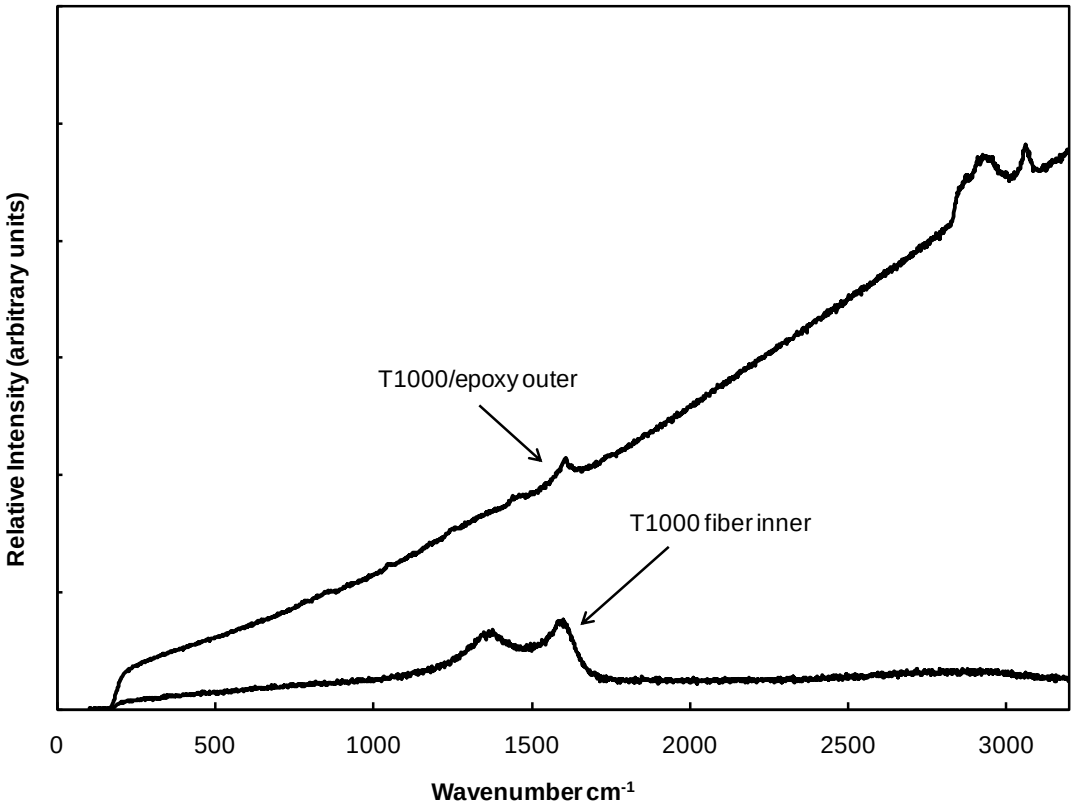

Figure 4-29. Raman spectra of T1000/epoxy burst tank samples showing measurements of the inner and outer portions of the tank using a 514 nm incident laser.

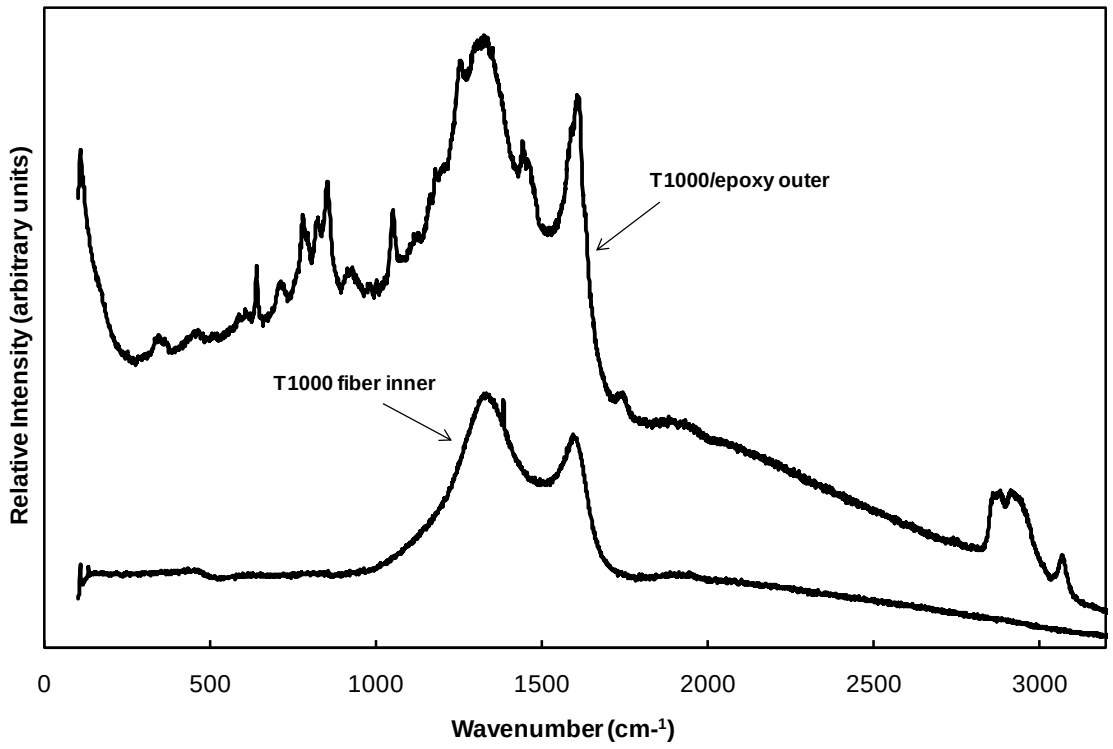

Figure 4-30. Raman spectra of T1000/epoxy burst tank samples showing measurements of the inner and outer portions of the tank using a 752nm incident laser.

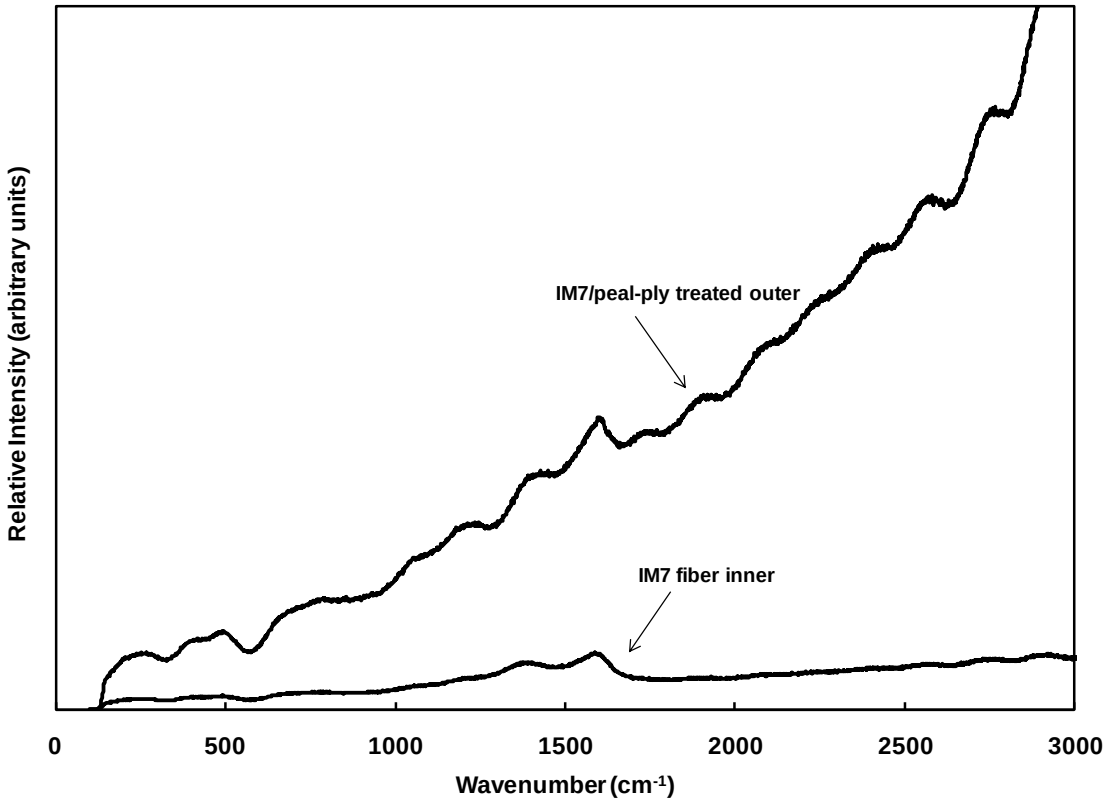

Figure 4-31. Raman spectra of IM7/epoxy with peal-ply treatment burst tank samples showing measurements of the inner and outer portions of the tank using a 488nm incident laser.

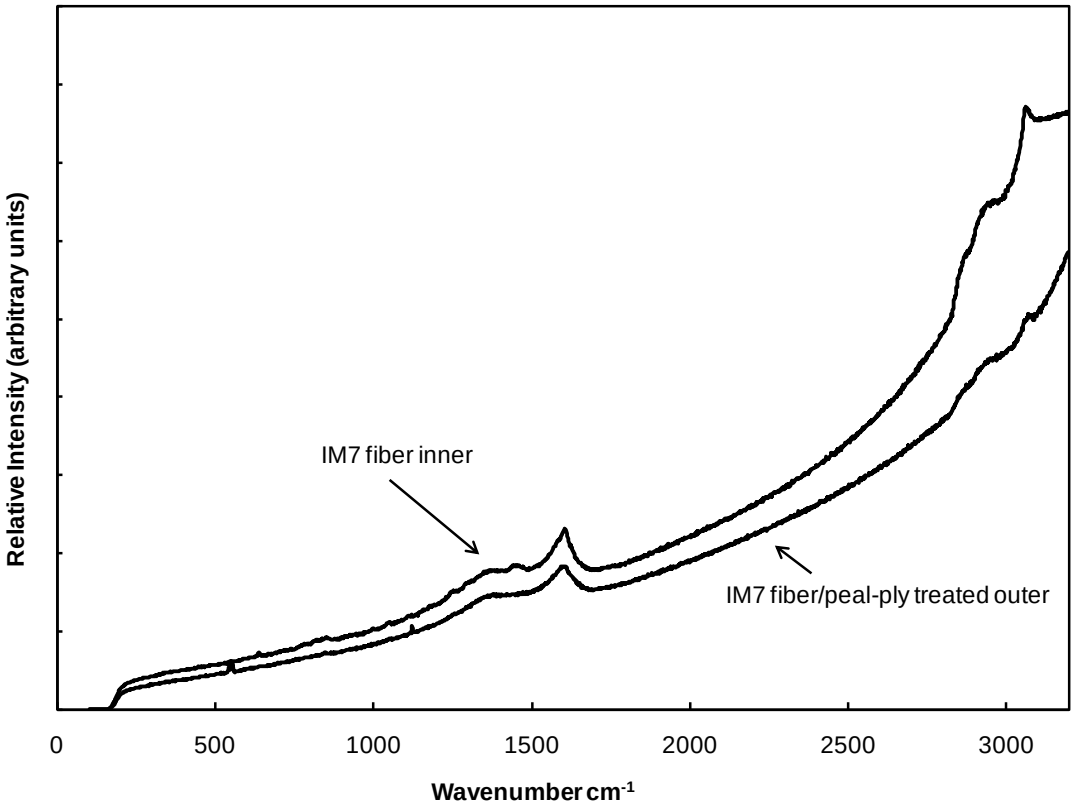

Figure 4-32. Raman spectra of IM7/epoxy with peal-ply treatment burst tank samples showing measurements of the inner and outer portions of the tank using a 514nm incident laser.

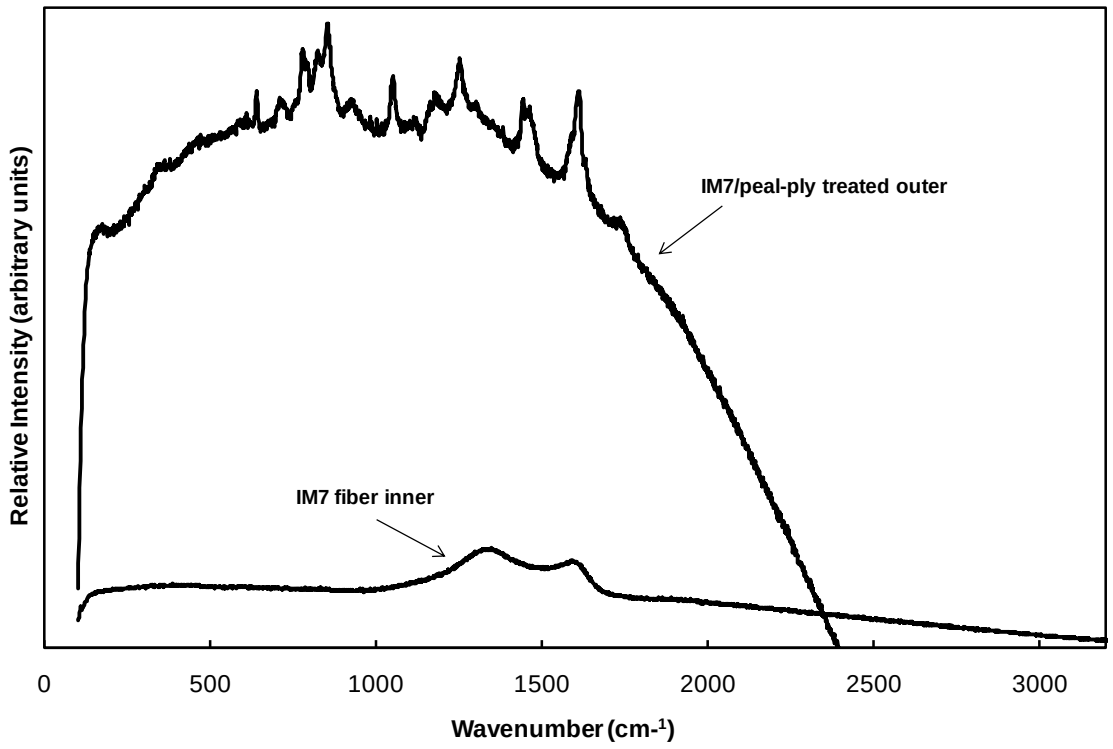

Figure 4-33. Raman spectra of IM7/epoxy with peal-ply treatment burst tank samples showing measurements of the inner and outer portions of the tank using a 752nm incident laser.

4.4 Data Summary and Discussion

From these exploratory tests on condition assessment of carbon fiber using Raman spectroscopy, much useful data has been compiled and analyzed. For all samples tested of both raw fiber and composite type, Raman bands as discussed in the literature section have been clearly identified and are reproducible. The incident laser wavelengths, laser power level, accumulation time, and range of wave-numbers investigated have been heavily varied in order to try to separate experimental artifacts from actual data that is measurement based. Software PeakFit® has been extensively used to quantify the

characteristics of these spectra and to form correlations with the changes as differential strain is applied using a load-frame.

With respect to the PAN-based fibers and their composites, many samples exhibit peak shifting of their two primary bands when undergoing applied strain. Specifically the T1000 fiber is discussed and carefully analyzed for its peak shifting characteristics. There exists a linear trend between applied strain and the location of both the G and D-band location. This value can vary from measurement to measurement due to experimental factors. During sampling the location of the laser must be moved every time the strain is adjusted, making it unable to measure the same fiber throughout the range of the strain test. Another reason the amount of peak shift may be different is that all the fibers are not at exactly the same strain. For higher-ordered bands no such strain relation could be clearly quantified. Additionally, the results from the PAN fibers showed that there is strong correlation between the FWHM ratio and intensity ratios and applied strain. The combination of these quantifiable peak characteristics is very important to establishing methods to evaluate these PAN-based carbon fiber composites.

For the pitch-based fibers, reproducible spectra were acquired with Raman peaks from the literature clearly identifiable. The pitch-based fibers did not exhibit a consistent peak shift with applied strain, although many of the samples spectra changed with applied strain. The structure and behavior of the pitch-based fibers is different than the PAN-based fibers. Pitch-based fibers are typically much stiffer and do not have as high of a tensile strength. This may

mean that pitch-based fibers should be evaluated and tested differently than PAN-based fibers to find out information about their structural integrity at a molecular level. More extensive testing should be done on these types of fibers.

For the composite materials Raman bands were found on all the material tested at each wavelength tested. The coating of the outside of the composite materials is often highly reflective making it difficult for the laser induced energy to penetrate the surface, especially with the shorter wavelength lasers. Using the longer wavelength 752nm laser to measure the material from the burst COPVs provides a much better response with more distinct Raman bands as shown in Figures 4-30 and 4-33 when compared to that of measurements using a 514nm incident laser. As with the other composite material, the spectra also contain an epoxy signature. Detailed analysis of the Raman spectra produced by the epoxies within these composite materials would be helpful.

5 CONCLUSIONS

5.1 Conclusions

Carbon fibers of pitch and PAN-based origins have been measured using a variety of incident lasers between 488 and 752 nm. For all materials tested, the D and G Raman bands can clearly be identified with each laser, with other fibers also having the D', and G' identified. Strain dependence of the D and G bands is demonstrated for the PAN-based fibers. Both the D and G bands have been found to decrease in resonance frequency as applied tensile strain increases. This observation is also supported in the literature by previous research in this field. From the initial results it appeared that the peak frequency decreased approximately 10 wave-numbers / percent applied strain. Additionally, from our results higher modulus and tensile strength PAN-based fibers exhibit a higher peak shift with applied strain. In our case the T1000 fiber typically had the highest peak shift. This is due to the higher degree of graphitization as previously discussed. The fibers that exhibited a peak shift also exhibited a decrease in FWHM and intensity ratio as strain level increases.

All the composite materials tested exhibited the D and G bands, as well as distinct epoxy signatures. This is important because it confirms that a Raman spectrometer with optimized system parameters has the ability to penetrate the

reflective coating on the outside of many composite materials. This is especially true at higher incident wavelengths because the laser has a greater penetration depth producing better results with more definite peaks. The future NDE applications in this field will likely be in the area of in situ Raman testing of the COPVs. This would be a practical and realistic approach for condition assessment of these materials.

In summary this project has come to the following conclusions.

- Raman spectroscopy has the ability to make measurements and detect distinct Raman bands related to molecular structure of the material on carbon fiber and carbon fiber composite materials.
- For some fiber and composite materials tested it is found that there is a peak shift with applied strain. Raman bands decrease in wavenumber with an increase in strain. In addition to shifting of Raman band location, relative FWHM and intensity ratios of fibers appear to decrease with an increase in applied strain.
- Raman spectroscopy can penetrate outer coatings of COPVs to make measurements detecting active Raman bands of carbon fiber and an epoxy matrix signature.

From this research and previous literature it is apparent that Raman spectroscopy has the ability to make measurements on carbon fiber and carbon fiber composites and could prove to be a valuable NDE tool for condition assessment of these materials.

5.2 Future Work

This project has made exploratory non-destructive attempts at characterizing and analyzing carbon fibers using Raman spectroscopy. The scope of this project mainly investigated PAN-based fibers and their Raman band location shifting with applied strain. Detailed strain testing should also be done on pitch-based carbon fibers, a more difficult process due to the stiffer nature of the material. The composites tested in this project all have an epoxy portion of their spectra, and detailed analysis of the Raman response of these epoxies would prove to be valuable for future advancements. The ability to quickly differentiate the carbon fiber and epoxy components of a spectrum would be beneficial for more analysis. Separating the carbon fiber portion of the spectrum out to analyze its bands would be most critical for monitoring structural integrity of composite materials.

REFERENCES

1. Chung, D., *Carbon Fiber Composites*. 1994, Newton, MA: Butterworh-Heinemann. 215.

2. Bacon, R., *Growth, Structure, and Properties of Graphite Whiskers.* Journal of Applied Physics, 1960. **31**(2): p. 283-290.

3. Morgan, P., *Carbon Fibers and their Composites*. 1 ed. 2005, Boca Raton, FL: CRC Press.

4. Tse-Hao, K., *Raman spectrum of modified PAN-based carbon fibers during graphitization.* Journal of Applied Polymer Science, 1996. **59**(4): p. 577-580.

5. Ferrar, J.R. and K. Nakamoto, *Introductory Raman Spectroscopy*. 1994, Boston: Academic Press, Inc. 370.

6. Weber, W.H. and R. Merlin, *Raman Scattering in Materials Science*. 1 ed. 2000, New York: Springer-Verlag. 492.

7. Brooks, T., *Condition Assesment of Kevlar Composite Materials using Raman Spectroscopy*, in *Department of Civil and Environmental Engineering*. 2007, University of Missouri: Columbia. p. 68.

8. Tuinstra, F., *Raman Spectrum of Graphite.* Journal of Chemical Physics, The, 1970. **53**(3): p. 1126.

9. Melanitis, N., *Characterization of PAN-based carbon fibres with laser Raman spectroscopy.* Journal of Materials Science (full set), 1996. **31**(4): p. 851.

10. Chaudhuri, S.N., et al., *Raman spectroscopy for characterization of interfacial debonds between carbon fibers and polymer matrices.* Composite Structures, 2006. **76**(4): p. 375-387.

11. Galiotis, C., *Strain dependences of the first-and second-order Raman spectra of carbon fibres.* Journal of Materials Science Letters, 1988. **7**(5): p. 545.

12. Wang, Y., D.C. Alsmeyer, and R.L. McCreery, *Raman spectroscopy of carbon materials: structural basis of observed spectra.* Chem. Mater., 1990. **2**(5): p. 557-563.

13. Washer, G. and F. Blum, *Raman Spectroscopy for the Nondestructive Testing of Carbon Fiber.* Research Letters in Materials Science, 2008.

14. Robinson, I.M., *Strain dependence of the Raman frequencies for different types of carbon fibres.* Journal of Materials Science Letters, 1987. **6**(10): p. 1212.

15. Sakata, H., *Effect of uniaxial stress on the Raman spectra of graphite fibers.* Journal of Applied Physics, 1988. **63**(8): p. 2769.

16. Amer, M.S., *Stress concentration phenomenon in graphite/epoxy composites: Tension/compression effects.* Composites Science and Technology, 1997. **57**(8): p. 1129.

17. Mitra, V.K., William M. Risen, Jr., and H.B. Ray, *A laser Raman study of the stress dependence of vibrational frequencies of a monocrystalline polydiacetylene.* The Journal of Chemical Physics, 1977. **66**(6): p. 2731-2736.

18. Wagner, H.D., *Residual Compression Stress Profile in High-Modulus Carbon Fiber Embedded in Isotactic Polypropylene by Micro-Raman Spectroscopy.* Applied Composite Materials, 2000. **7**(4): p. 209.